Ci 13
(308/1961)

UDC 624.5:534.1

ACTA POLYTECHNICA SCANDINAVICA

CIVIL ENGINEERING AND BUILDING CONSTRUCTION SERIES No. 13

ARNE SELBERG

Oscillation and Aerodynamic Stability of Suspension Bridges

Norwegian Contribution No. 13

Trondheim 1961

ACTA POLYTECHNICA SCANDINAVICA

. . . a Scandinavian contribution to international engineering sciences

Published under the auspices of the Scandinavian Council for Applied Research

in Denmark by the Danish Academy of Technical Sciences

in Finland by the Finnish Academy of Technical Sciences, the Swedish Academy of Engineering Sciences in Finland, and the State Institute for Technical Research

in Norway by the Norwegian Academy of Technical Science and the Royal Norwegian Council for Scientific and Industrial Research

in Sweden by the Royal Swedish Academy of Engineering Sciences, the Swedish Natural Science Research Council, and the Swedish Technical Research Council

Acta Polytechnica Scandinavica is divided into the following sub-series:

Chemistry including Metallurgy Series, Ch
Civil Engineering and Building Construction Series, Ci
Electrical Engineering Series, El
Mathematics and Computing Machinery Series, Ma
Mechanical Engineering Series, Me
Physics including Nucleonics Series, Ph

For subcription to the complete series or to one or more of the sub-series and for purchase of single copies, please write to

ACTA POLYTECHNICA SCANDINAVICA PUBLISHING OFFICE
Box 5073
Stockholm 5
Sweden **Phone 67 09 10**

This issue is published by
NORGES TEKNISKE VITENSKAPSAKADEMI
Trondheim, Norway

and is designated as NTVA Publication series 1, No. 11, 1961.
Editor: Knut Alming

Ci 13
(308/1961)

UDC 624.5:534.1

ACTA POLYTECHNICA SCANDINAVICA

CIVIL ENGINEERING AND BUILDING CONSTRUCTION SERIES No. 13

ARNE SELBERG

Oscillation and Aerodynamic Stability of Suspension Bridges

Norwegian Contribution No. 13

Trondheim 1961

N.T.H. Trykk

Trondheim 1961

Contents.

Introduction			I
Notations			IV
1.	Basic equations for vertical oscillations	p.	1
1.1	Deducion of differential equations	"	1
1.2	Effect of hanger inclination	"	6
2.	Natural frequencies in vertical oscillations	"	10
2.1	Single span bridge	"	10
2.1.1	Symmetric oscillations	"	15
2.1.2	Antimetric oscillations	"	15
2.2	Symmetrical three span bridge	"	16
2.2.1	Symmetric oscillations	"	18
2.2.2	Antimetric oscillations	"	20
2.3	Two span bridge	"	26
3.	Natural frequencies in torsional oscillations	"	26
3.1	Deduction of equations	"	26
3.2	Torsional stiffness and warping	"	28
4.	Effect of lateral static wind forces	"	33
5.	Effect of simplifications	"	35
5.1	Shear deformation in stiffening truss	"	35
5.2	Cable force	"	35
5.3	Cable slope	"	36
5.4	Lateral movements	"	36
6.	Model tests for suspension bridges	"	37
6.1	Models and model dimensions. Damping	"	37
6.2	Full model and sectional model	"	38
6.3	Mounting of model	"	40
7.	Test results	"	43
7.1	Systematic tests with simplified models	"	43
7.2	Coupeled oscillations. Flutter velocity	"	43
7.3	Coupeled oscillations. Critical velocity	"	46
7.4	Vertical oscillations	"	55
7.5	Effect of structural damping	"	59
7.6	Concluding remarks	"	60
7.7	Numerical example	"	61

8. Natural wind and wind forces p. 64
8.1 Nature of wind " 64
8.2 Design wind velocity " 65
9. References " 67
10. Summary " 69

Introduction.

Since the disaster in 1940 with the Tacoma Narrow's Bridge, the investigation of the aerodynamic stability of suspension bridges has been in the centre of interest for bridge builders and scientists, and the scope of numerous treatises. The disaster of the Tacoma Narrow's Bridge was not the only example of trouble with the suspension bridges, and the result of the work done since 1940 demonstrates clearly that numerous bridges are not aerodynamic stable for all wind conditions. However, the bridges demonstrate that a soundly constructed suspension bridge will stand severe oscillations for a considerable time without any serious trouble, and there is numerous examples of minor oscillations being entirely harmless to the bridge.

For new bridges there is no reason for allowing any severe oscillations. For the trafficants all oscillations will be unpleasant and give a feeling of insecurity. However, if we demand that the bridge in very heavy storms, which will occure only with intervals of years, shall be safe against any damages and for a usual storm only exhibit small and unharmful oscillations, this should be sufficient for all public use of a bridge.

It is very important to find easy and quick methods which can give critical wind velocities and oscillation amplitudes with a sufficient accuracy. This is especially of importance in the early stages of planning and design of the bigger suspension bridges and will give information about alternatives which are worth a more complete investigation.

When planning a greater suspension bridge it will be natural to take a control of the preliminary investigations by testing a model in a windtunnel. However, when designing middle or small span suspension bridges the preliminary investigations should be sufficiently accurate and a testing of models superfluous.

The scope of this paper is to give a tool for such a preliminary investigation of the aerodynamic stability.

The author believes that for most bridges the results obtained will be sufficiently accurate to make investigations with a model unnecessary.

Another and very important result of a quick preliminary investigation of the aerodynamic stability will be that it is readily seen how and where the structure may be improved, and thus making it possible to produce better and safer bridges without any great increase in cost.

The usual model will be a cross-sectional model, see f. inst. fig. 22 and 23. A better model would be a model of the complete bridge. However, complete models cost too much and working with them takes considerable time.

The main cause of errors with the wind tunnel test is the wind itself. The natural wind will be turbulent and changing in velocity and direction. It seems to be impossible to produce such a wind in a wind tunnel. The only model giving correct results is the bridge itself. However, all the investigations on models and bridges done in the years after 1940 clearly demonstrate that there is a correlation between the behaviour of bridge and model. There is never reported trouble with a bridge which gives good model tests, and for several bridges there has been a possibility to compare the oscillations in bridge and model in detail. The model will not give a complete and in all correct picture of how the bridge behaves, but it gives a sufficiently good picture for a predicting of how the bridge will stand the wind and what will be the critical wind velocity.

The paper gives in the first part a deduction of fundamental equtations and a deduction of natural frequencies, including effects as inclination of hangers and other secondary effects. The inclination of hangers may for some bridges be of great importance and gives a marked effect on the frequency, see f. inst. fig. 5.

The frequencies are calculated for bridges with 1, 2 or 3 spans, and for vertical or torsional oscillations. Effects of lateral wind forces and various simplifications are briefly investigated, and a short introduction in model theory is given in Chapt. 6.

The test results and diagrams are given in Chapt. 7. They represent the results of numerous tests done by the civil engineers Bernt Skjeggestad, Bjørn Vik, Olav Mo, Øivind Iveland and T. C. Haug during the years 1954 - 58. The author wishes to express his gratitude for their assistances.

The use of the test results is simplified by using the flutter velocity, Chapt. 7.2 as a reference value for coupled and torsional oscillations. The flutter velocity V_F may be found from the diagram, Fig. 25 or still simpler by an empirical formula (7.1). The critical wind velocities for the actual bridge are found by multiplying the flutter velocity V_F with coefficients given

in diagrams Fig. 30 - 38 for coupled oscillations. For pure vertical oscillations a similar method is used, see diagrams Fig. 42 - 44.

In Chapt. 7.3 and 7.4 is given a definition of various types of oscillations and the comparing critical wind velocities.

It is the hope of the author that the sceptisism against suspension bridges, a result of the Tacoma Bridge disaster, in time will be conquered. To-day numerous papers giving the theory and results of investigations on the aerodynamic stability exist.

When the Tacoma Bridge disaster occured, the knowledge of these problems among bridge designers was almost zero. The lessons of the many disasters in the last century had been forgotten.

To-day the investigation of aerodynamic stability should be a self-evident part of the design of any suspension bridges. In the opinion of the author a sufficiently accurate value of the critical wind velocity for most bridges may be found with use of the diagrams presented here.

A great part of the tests referred to in this paper was done on behalf of the Norwegian Administration of Public Roads and the Printing of the paper is made possible by the assistance of Norges Teknisk-Naturvitenskapelige Forskningsråd, I wish to express my gratitude for their help and financial assistance.

Trondheim, 1/9 - 1960

Arne Selberg

Notations.

The notations are usually defined when they are first introduced. A survey of the notations and where they are introduced is given below.

A ; A_t	Axial force in stiffening truss. Chapt. 1. Fig. 2.
A_c	Cross-section of cable. Chapt. 1.1. Fig. 1 - 2.
A_1 ; A_2	Area of upper and lower chord of stiffening
A_u ; A_l	truss. Chapt. 3.2. Figs. 15, 17, 19.
A_D, A_V, A_C	Areas of diagonals, verticals and cross beams in truss systems. Chapt. 3.2. Fig. 17.
B	Shortening. Chapt. 1.2. Eq. (1.14)
C	Shortening. Chapt. 1.2. Eq. (1.14)
C_w	Warping modulus. Chapt. 3. Eq. (3.1, 3.20)
D	Shortening. Chapt. 2.3. Eq. (2.36)
D_a	" " 2.2.2. Eq. (2.31)
D_s	" " 2.2.1. Eq. (2.25)
E	Modulus of elasticity for stiffening truss.
E_c	Modulus of eleasticity for cable.
$F(x,t)$	Functions. Chapt. 1.1. Eq. (1.1 - 1.8)
G	Shear modulus.
H ; H_t	Horizontal component of cable force. Fig. 2.
$\bar{H}$	$H.\sec\varphi_m$. Chapt. 2. Eq. (7b).
H_w	Horizontal component due to dead load. Fig. 2.
H_s	Horizontal component due to live load or mass forces
ΔH	Effect of hanger inclination. Chapt. 1.2. Eq. (1.13)
I	Stiffening truss modulus of inertia. Fig. 1 - 2.
I_D	Modulus of torsion. Eq. (3.1 ; 3.20)
K_1 ; K_2	Coefficients concerning effect of hanger inclination. Eq. (1.14)
L_s	Function of cable length. Eq. (2.8)

M_1 ; M_t	Bending moment
M_c	Total mass of cable within a span. Chapt. 1.2. Fig. 6.
M_g	$m_g \cdot l$ mass of suspended structures within a span. Chapt. 2.2.1. Eq. (2.5a)
M_p	Mass. Chapt. 2.2.2. Eq. (2.23)
$\mathcal{M}$	$\int r^2 dm$ Chapt. 3.1. Eq. (3.3)
N	Axial Force. Chapt. 3.2. Fig. 16.
N	Frequency = $\frac{1}{T}$ Chapt. 6.1. Eq. (6.2)
S(x, t)	Hanger force pr. unit length. Chapt. 1.1. Eq. (1.1)
S_1 ; S_2	Spring constants. Chapt. 6.3. Fig. 23.
T	Time for one cycle. Chapt. 2. Eq. (2.1)
T	as index means torsion
V	Shear force
a	Coefficients. Chapt. 2. Eq. (2.9)
a	Amplitude. Chapt. 7. Eq. (7.7)
a	Acceleration. Chapt. 6. Eq. (6.1)
b	Distance between trusses. Fig. 14, 15 and 17.
b	Bridge width. Chapt. 7. Fig. 24.
d	Bridge depth. Chapt. 7. Fig. 24.
f; f_1; f_2	Cable sag. Figs. 1 - 9.
h ; h(x)	Hanger length. Fig. 1 ; 2.
l ; l_1 ; l_2	Span length. Fig. 1 ; 9.
m ; m_1 ; m_2	Mass pr. unit length and pr. cable.
m_c	Mass pr. unit length of cable.
m_g	Mass pr. unit length of girder etc.
m	used as index for model. Chapt. 6.
n	index giving number in series.
t	Time, as index function of time.

v ; v_1 ; v_2 ; v_3	Wind velocity. Chapt. 7.
v_c	Critical wind velocity. Chapt. 7. Eq. 7.2.
v_F	Flutter velocity. Chapt. 7. Eq. 7.1.
v	as index means vertical
x	Abscissae
y	Ordinate.
α ; α_1 ; α_2	Shortening. Chapt. 2.1. Eq. (2.14)
α_T	" Chapt. 3.1. Eq. (3.8)
α	Angel of wind attack. Chapt. 7. Figs. 26 - 38.
β ; β_1 ; β_2	Shortening. Chapt. 2.1. Eq. (2.14)
β_T	" Chapt. 3.1. Eq. (3.8)
γ_t ; γ	Longitudinal movement of truss. Fig. 2.
δ	Decrement. Structural damping.
ε	Shortening. Chapt. 2.1. Eq. (2.12)
ζ	" Chapt. 3.2. Eq. (3.15)
η_t ; η	Vertical deflection of cable and truss. Fig. 2.
ϑ	Shortening. Chapt. 2.2.2. Eq. (2.31)
θ	Symbol for shear resistance. Chapt. 3.2. Eq. (3.10) and (3.22)
$\varkappa$	Shortening. Chapt. 2.1. Eq. (2.14)
$\varkappa_T$	" " 3.1. Eq. (3.8)
λ ; λ_1 ; λ_2	" " 2.1. Eq. (2.14) ; (2.26) ; (2.33)
λ_T	" " 3.1. Eq. (3.8)
μ	" " 2.2.2. Eq. (2.31)
μ_T	" " 3.1. Eq. (3.8)
μ	Shortening for mass relations. Chapt. 7. Fig. 25.
ν	Preform of stiffening truss. Fig. 1.
ν_n	Preform of stiffening truss at $x = \frac{1}{2}l$.
ν	Mass radius of gyration. Chapt. 7. Eq. (7.1), Fig. 25.

ξ Longitudinal movement of cable. Fig. 2.

ξ_p Longitudinal movement of cable saddle. Eq. (2.22)

φ Cable slope for dead load. Fig. 2.

ϕ Angle of torsion. Chapt. 3.1. Chapt. 7.3.

ψ Cable slope in deflected bridge. Fig. 2.

1. BASIC EQUATIONS FOR VERTICAL OSCILLATIONS.

1.1. Deduction of differential equations.

In order to simplify the mathematical treatment of the oscillating system, the following assumptions are made:

1. Axial deformations of towers and suspenders may be neglected.
2. The distance between the suspenders is small compared to the span width l, and the suspenders may be replaced by a membrane without resistance to shear.
3. For dead load only the cable curve is a parabola.
4. The stiffness lE of the stiffening girder or truss is constant within the span length l. The spacing of the stiffening truss is small compared to the span length l.
5. The curve of the stiffening truss is small compared to the cable curve. See Fig. 1.

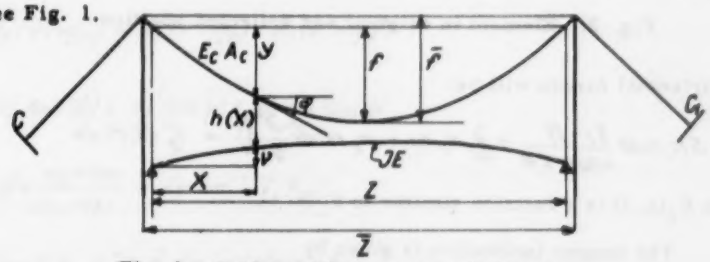

Fig. 1. Bridge with one suspended span.

6. There is no live load or traffic load on the oscillating bridge.

This assumptions are except for the last one the same as usual in the static investigation of suspension bridges. For the lower frequensies, which are of interest, the assumptions are fully justified.

If we consider an element dx of the oscillating bridge, Fig.'s 1 and 2, the cable element will have the vertical forces

$$S(x,t)dx + w_c(x) + \frac{d}{dx}(H_t \tan\psi)dx - m_c(x)dx\frac{\partial^2 v}{\partial t^2} = F_1(x,t)dx \qquad (1)$$

where S(x, t) is the hanger force, $w_c(x)$ the weight and $m_c(x)$ the mass of the cable - all pr. unit length. H_t is the horizontal component of the cable force. $F_1(x, t)$ is a function which stands for eventual wind forces and aerodynamic and structural damping.

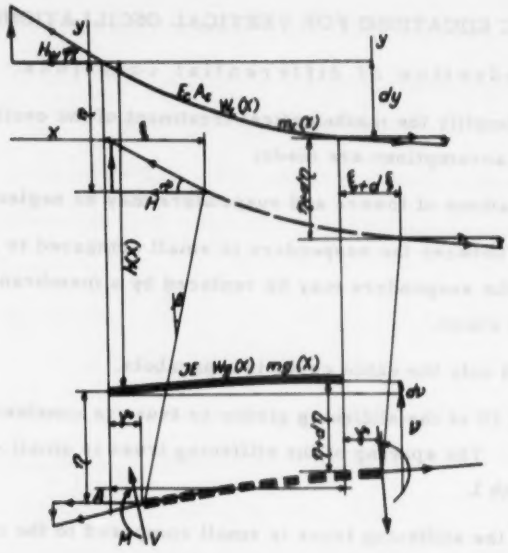

Fig. 2. Element in original and deflected position.

The horizontal forces will be:

$$-S(x,t)\,dx\,\frac{\xi_t-\gamma_t}{h(x)\cos\beta}+\frac{\partial}{\partial x}H_t\,dx-m_c(x)\,dx\,\frac{\partial^2\xi_t}{\partial t^2}=F_2(x,t)\,dx \qquad (2)$$

Where $F_2(x, t)$ is a function similar to $F_1(x, t)$.

The hanger inclination is given by

$$\tan\beta=\frac{\xi_t-\gamma_t}{h(x)\cos\beta}$$

see Fig. 2. Usually we have $\cos\beta\approx 1$.

For an element of the suspended structure we get similarly:
Vertical forces:

$$w_g(x)\,dx-S(x,t)\,dx+\frac{\partial V_t}{\partial x}dx+\frac{\partial}{\partial x}\left(A_t\left(\frac{\partial v}{\partial x}+\frac{\partial \eta_t}{\partial x}\right)\right)dx-m_g(x)\,dx\,\frac{\partial^2\eta_t}{\partial t^2}=F_3(x,t)\,dx \qquad (3)$$

Horizontal forces:

$$\frac{\partial}{\partial x}A_t\,dx-\frac{\partial}{\partial x}\left(V_t\left(\frac{\partial v}{\partial x}+\frac{\partial \eta_t}{\partial x}\right)\right)dx+m_g(x)\,dx\,\frac{\partial^2\gamma_t}{\partial t^2}+S(x,t)\,dx\,\frac{\xi_t-\gamma_t}{h(x)\cos\beta}=F_4(x,t)\,dx \qquad (4)$$

where A is the horizontal component of axial force in the stiffening girder and V_t is the shear force.

Equations (1) and (3) reduce to

$$w(x)\,dx+\frac{\partial}{\partial x}(H_t\tan\psi)\,dx+\frac{\partial}{\partial x}V_t\,dx+\frac{\partial}{\partial x}\left(A_t\left(\frac{\partial v}{\partial x}+\frac{\partial \eta_t}{\partial x}\right)\right)dx-m(x)\,dx\,\frac{\partial^2\eta_t}{\partial t^2}=F_5(x,t)\,dx$$

Shear and moment are connected by:

$$\frac{\partial}{\partial x} M_f \, dx = V_f \, dx$$

Deflection, moment and shear are connected by

$$\frac{\partial^2}{\partial x^2} \eta_f = -\frac{M_f}{JE} + \frac{\frac{\partial}{\partial x} V_f}{\frac{1}{\chi} GF} \tag{5}$$

The last term may usually be neglected. It is of importance only for the higher modes and is investigated in Chapt 5.1.

Introducing $\frac{\partial V_f}{\partial x} = -JE \frac{\partial^4 \eta_f}{\partial x^4}$ and writing

$\frac{\partial x}{\partial x} = \eta'$; $\frac{\partial \eta}{\partial t} = \dot{\eta}$ we get

$$w(x) - JE \eta_f'''' - \frac{\partial}{\partial x}(A_f(v'+\eta_f')) + \frac{\partial}{\partial x}(H_f \tan\psi) - m(x)\ddot{\eta}_f = F_I(x,t) \tag{6}$$

where

$$\frac{\partial}{\partial x}(A_f(v'+\eta_f')) = A_f'(v'+\eta_f') + A_f(v''+\eta_f'')$$

$$\frac{\partial}{\partial x}(H_f \tan\psi) = H_f' \tan\psi + H_f \frac{\partial}{\partial x} \tan\psi$$

$$\tan\psi = \frac{dy+d\eta_f}{dx+d\xi_f} = (y'+\eta_f')(1-\xi_f')$$

$$\frac{\partial}{\partial x} \tan\psi = y'' + \frac{\partial}{\partial x}(\eta_f' - (y'+\eta_f')\xi_f')$$

The horizontal component of cable force will be

$$H_f = H_w + H_{sf} \text{ , where } H_{sf} = H_{sf\,x=0} + \int_0^x H_f' \; ; \; H_f' = H_{sf}'$$

and $H_w = -\frac{w(x)}{y''}$

H_w being the horizontal component of cable force for dead load only.

Similarly for the stiffening girder

$$A_f = A_{f\,x=0} + \int_0^x dA_f$$

Consequently Eq. (6) will be written

$$JE \eta_f''' - H_{sf} y'' - H_f \frac{\partial}{\partial x}(\eta_f' \sec^2\varphi) - H_{sf}' y' - A_f(v''+\eta_f'') - A_f'(v'+\eta_f') + m(x)\ddot{\eta} = F_I(x,t) \tag{7}$$

In Eq. (7) is used the simplification

$$\eta_t' - (y' + \eta_t')\xi_t' \approx \eta_t' - y'\xi_t' \approx \eta_t' + y'^2\eta_t' = \eta_t' \sec\varphi$$

See Eq. (10a).

In the same manner Eq's (2); (4) result in

$$H_{st}' + A_t' + \frac{\partial}{\partial x}(JE\eta_t''' (v' + \eta_t')) - m_c(x)\ddot{\xi}_t - m_g(x)\ddot{y}_t = F_{II}(x,t) \tag{8}$$

And similarly Eq's (1); (2)

$$H_{st}'\left(1 - \tan\psi \frac{\bar{y}_t - \xi_t}{h(x)\cos\beta}\right) - \left(H_t \frac{\partial}{\partial x}\tan\psi + w_c(x)\right)\frac{\bar{y}_t - \xi_t}{h(x)\cos\beta}$$

$$- m_c(x)\left(\ddot{\xi}_t - \ddot{\eta}_t \frac{\bar{y}_t - \xi_t}{h(x)\cos\beta}\right) = F_2(x,t) - F_1(x,t)\frac{\bar{y}_t - \xi_t}{h(x)\cos\beta} \tag{9}$$

To obtain an equation between η and ξ we use the deformations of a cable element.

In the undeformed state we have

$$(dL)^2 = dx^2 + dy^2$$

and similarly in the deflected state

$$(dL + \Delta dL)^2 = (dx + d\xi_t)^2 + (dy + d\eta_t)^2$$

The terms ΔdL^2 and $d\xi^2$ will be small of higher order, consequently

$$d\xi_t = \frac{\Delta dL \cdot dL}{dx} - \frac{dy \cdot d\eta_t}{dx} - \frac{1}{2}\frac{d\eta_t^2}{dx}$$

The elongation ΔdL of the cable element will be

$$\Delta dL = \frac{H_t\, dL}{E_c A_c}\sec\psi - \frac{H_w\, dL}{E_c A_c}\sec\varphi \;; \quad dL = dx\sec\varphi$$

and

$$\xi_t' dx = \frac{H_t}{E_c A_c}\sec^2\varphi \cdot \sec\psi\, dx - \frac{H_w}{E_c A_c}\sec^3\varphi\, dx - y'\eta_t' dx - \frac{1}{2}(\eta_t')^2 dx \tag{10}$$

Simplified to the dominating term

$$\xi_t' dx \approx -y'\eta_t' dx \tag{10a}$$

The longitudinal displacement of a cable is

$$\xi_{tB} = \int_C^B \frac{H_t \sec^2\varphi \cdot \sec\psi}{E_c A_c} dx - H_w \int_C^B \frac{\sec^3\varphi}{E_c A_c} dx - \int_C^B y'\eta_t' dx - \frac{1}{2}\int_C^B (\eta_t')^2 dx$$

Integrating from an anchorage C to a point B. Integrating between the anchorages we have

$$\int_0^l y'\eta_1'\,dx = \left[y'\eta_1\right]_0^l - y''\int_0^l \eta_1\,dx = -y''\int_0^l \eta_1\,dx$$

$$\sec^2\varphi = 1+(y')^2 \;;\quad \sec\varphi \approx 1+\tfrac{1}{2}(y')^2$$

$$\sec\psi = \sqrt{1+((y'+\eta_1')\cdot(1-\xi_1'))^2} \approx 1+\tfrac{1}{2}(y'+\eta_1')^2$$

$$\int_C^{C'} \frac{H_{st}\sec^2\varphi\cdot\sec\psi}{E_c A_c}\,dx - H_w\int_C^{C'}\frac{\sec^3\varphi}{E_c A_c}\,dx = \int_C^{C'}\frac{H_{st}\sec^2\varphi\cdot\sec\psi}{E_c A_c}\,dx + \frac{H_w}{E_c A_c}\,y''\int_0^l \eta_1\,dx$$

The equation will be:

$$\xi_{C'} = 0 = \int_C^{C'}\frac{H_{st}\sec^2\varphi\cdot\sec\psi}{E_c A_c}\,dx + \frac{H_w}{E_c A_c}\,y''\int_0^l \eta_1\,dx + y''\int_0^l \eta_1\,dx - \frac{1}{2}\int_0^l(\eta_1')^2\,dx$$

As $E_c A_c$ will be great compared to H_w the second term may be neglected, giving an error of the magnitude 1 o/oo to 3 o/oo for various bridges [10]. Similarly the term

$$\int_C^{C'}\frac{H_{st}\sec^2\varphi\cdot\sec\psi}{E_c A_c}\,dx \approx \int_C^{C'}\frac{H_{st}\sec^3\varphi}{E_c A_c}\,dx$$

give by the simplification an error of the same magnitude. We get

$$\int_C^{C'}\frac{H_{st}\sec^3\varphi}{E_c A_c}\,dx + y''\int_0^l \eta_1\,dx - \frac{1}{2}\int_0^l(\eta_1')^2\,dx = 0 \qquad (11a)$$

The last erm, usually being of minor importance [10], may be neglected,

$$\int_C^{C'}\frac{H_{st}\sec^3\varphi}{E_c A_c}\,dx + y''\int_0^l \eta_1\,dx = 0 \qquad (12)$$

Equation (12) is except for the variable cable tension H_{st}, identical with the usual cable equation. The effect of neglecting the last term in Eq.(11a) is discussed in Chapt. 5. 2.

1.2. Effect of hanger inclination.

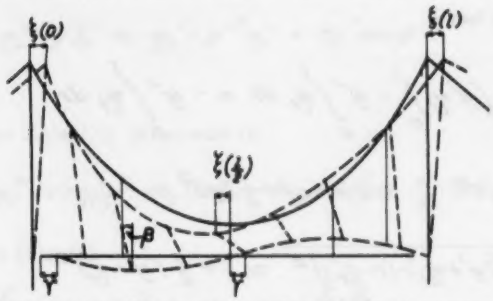

Fig. 3. Inclination of hangers and longitudinal movement.

The deflections in a span, Fig. 3., result in a variable cable force, see Fig. 4.

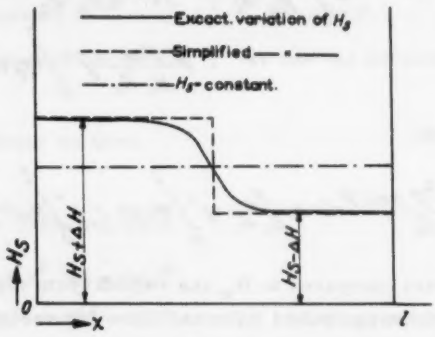

Fig. 4. Variation of cable force due to the hanger inclination.

With small deflections we usually have $\cos\beta \approx 1$, and a calculation with $\cos\beta = 1$ will be sufficiently correct. Fig. 5 demonstrates the correctness of this assumption. The agreement between calculated and observed time for an oscillation in 2 half waves is extremely good for all normal proportions $h(l/2)/l$ or $h(l/2)/f$.

With increasing oscillations we have $\cos\beta < 1$, however, the effect is small as easily is demonstrated on a model, in fact it is difficult to observe the slight increase in frequency following increasing amplitudes.

The actual variation of H will in this paper be replaced by the simplified variation shown in Fig. 4. [1].

From Equation (2) we have

$$\frac{\partial H_t}{\partial x}dx = -w_c(x)dx\ddot{\xi}_t - S(x,t)dx\frac{\xi_t - \xi_r}{h(x)}$$

introducing $\cos\beta \approx 1$. $S(x, t)$ is the hanger force.

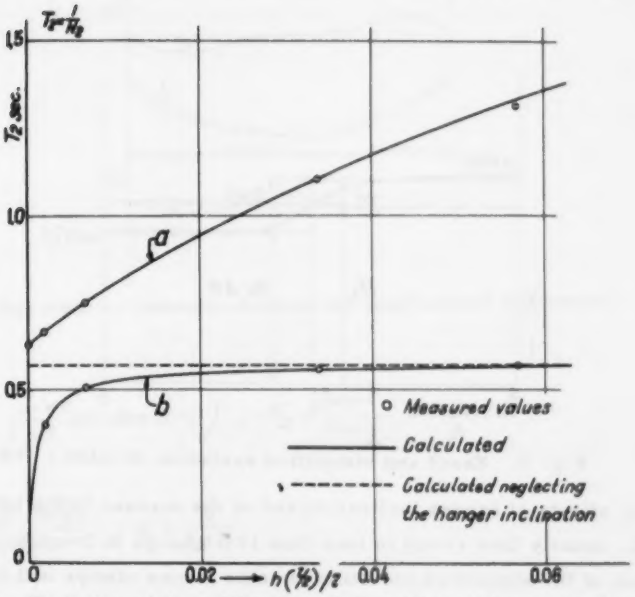

Fig. 5. Experimental verification of the effect of hanger inclination. Calculated and measured time for one cyclus.

The distribution of cable masses $m_c(x)$ are replaced by a simplified system, see Fig. 6.

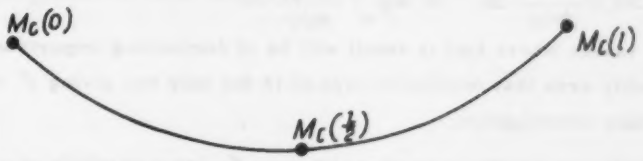

Fig. 6. Simplified distribution of cable masses. Longitudinal movement.

Where

$$M_c(0) = \frac{1}{4} M_c \; ; \; M_c(\tfrac{1}{2}) \approx \frac{1}{2} M_c \quad \text{and} \quad M_c(l) \approx \frac{1}{4} M_c$$

M_c is the total mass of cable within the span l.

The variation in cable force is replaced by the steps in Fig.'s 4 ; 7. Where

$$2\Delta H_f = -\frac{1}{2} M_c \ddot{\eta}_f\left(\frac{l}{2}\right) - \int_0^l S(x,f)\,\frac{\eta_f - \gamma_f}{h(x)}\,dx$$

$$\Delta H(0)_f = -\frac{1}{4} M_c \ddot{\eta}_f(0) \quad ; \quad \Delta H(l)_f = -\frac{1}{4} M_c \ddot{\eta}_f(l) \qquad \Big\} \quad (13)$$

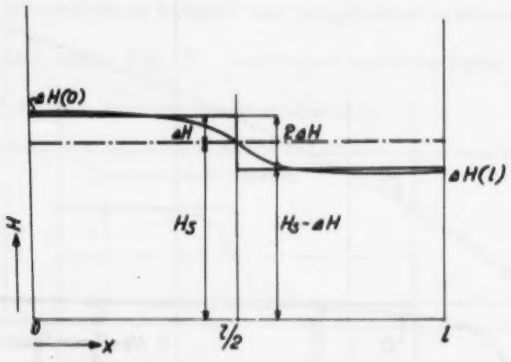

Fig. 7. Exact and simplified variation of cable force.

As the effects of hanger inclination and of the masses in the cables are small, usually they result in less than 10% change in frequencies, the introduction of the simplified variation of cable forces always will be sufficiently accurate, reducing the errors to less than 2%.

Fig. 8 gives the variation of η for various types of oscillations. In the integral

$$\int S(x,f)\,\frac{\eta_f - \gamma_f}{h(x)}\,dx \approx w_g \int \frac{\eta_f - \gamma_f}{h(x)}\,dx$$

the values where h(x) is small will be of dominating importance, and it is readily seen that oscillation type a) is the only one giving η values worth a further investigation.

Introducing for this type of oscillation, η_f as a parabola of second order, we get

$$\int_0^l S(x,f)\,\frac{\eta_f - \gamma_f}{h(x)}\,dx \approx w_g \int_0^l \frac{\eta_f - \gamma_f}{h(x)}\,dx = 2\left\{K_1 \eta_f\left(\frac{l}{2}\right) - K_2 \gamma_f - (K_1 - K_2)\frac{1}{2}\left(\eta_f(0) + \eta_f(l)\right)\right\} \quad (14)$$

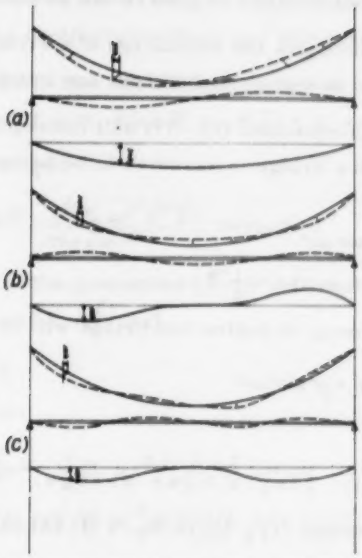

Fig. 8. Intercourse between vertical and longitudinal movement.

where

$$K_1 = \frac{w_g l}{2h(\frac{1}{2})}\left(\frac{1+C}{B}\arctan B - C\right) \; ; \; K_2 = \frac{w_g l}{2h(\frac{1}{2})}\,\frac{\arctan B}{B}$$

$$B = \sqrt{\frac{h(o) - h(\frac{1}{2})}{h(\frac{1}{2})}} \; ; C = \frac{1}{B^2}$$

h(o) and $h(\frac{1}{2})$ are the length of hangers at towers and midspan respectively. The expression for effect of hanger inclination as given above, is a very accurate one. This may be confirmed by comparison with the results of a numerical integration or with the results of systematic tests, see Fig. 5.

(14)

2. NATURAL FREQUENCIES IN VERTICAL OSCILLATIONS.

In the following we investigate the oscillation of a bridge with Zero aerodynamic and structural damping, and without any impulse from wind etc.

The functions F(x, t) in equations (1) - (9) will consequently all be Zero. The oscillation of such a bridge is assumed to be harmonic and represented by [2 , 13]

$$\eta_t = \eta \sin 2\pi \frac{t}{T} = \eta \sin \omega t \tag{1}$$

where η is the deflection at $t = \frac{1}{4} T$.

The longitudinal movement of cables and bridge will be

$$\xi_t = \xi \sin \omega t \quad ; \quad \gamma_t = \gamma \sin \omega t \tag{2}$$

respectively.

2.1. Single span bridge, Fig. (1).

Introducing the expressions (1) ; (2) in Eq. 's (1.13) and (1.14) we get

$$2\Delta H_t = \left[\frac{1}{2} M_c \omega^2 \xi\left(\frac{l}{2}\right) - \int_0^l S(x,t) \frac{\xi - \gamma}{h(x)} dx\right] \sin \omega t$$

$$2\Delta H_t = 2\Delta H \sin \omega t = \left[\frac{1}{2} M_c \omega^2 \xi\left(\frac{l}{2}\right) - 2\left\{K_1 \xi\left(\frac{l}{2}\right) - K_2 \gamma\right\}\right] \sin \omega t \tag{3}$$

The terms containing $\xi(0)$ and $\xi(l)$ being of no importance in a one span bridge.

The horizontal forces acting on the stiffening girder are given in Eq. (1.4), where $\cos\beta \approx 1$, F(x, t) = o. Further on we have that the term

$\frac{\partial}{\partial x}(V_t(v' + \eta'))\, dx$ always may be neglected as small.

With an effect of hanger inclination as demonstrated in Fig. 's (4) and (7) we get:

$$\frac{\partial}{\partial x} A_t\, dx - m_g(x) dx \ddot{\xi}_t = 0$$

and

$$\left.\begin{aligned} A_t &= A \sin \omega t = (-m_g \omega^2 \gamma x + A_{(0)}) \sin \omega t \; ; && (0 \le x \le \tfrac{l}{2}) \\ A_t &= A \sin \omega t = (-m_g \omega^2 \gamma x + A_{(0)} - 2\Delta H + \tfrac{1}{2} M_c \omega^2 \xi(\tfrac{l}{2})) \sin \omega t \; ; && (\tfrac{l}{2} \le x \le l) \end{aligned}\right\} \tag{4}$$

Δ H is given in Eq. (3).

If the bridge can move on the bearings at both ends we have $A(o) = -A(l) \approx 0$, as we investigate an oscillation without any frictional damping.

The other possibility is that the stiffening truss is hindered in longitudinal movement at one end f. inst. $A(o) \gtrless o$, $A(l) = o$, and $\gamma = o$.

With no hindering we get

$$\gamma_1 = \gamma \sin \omega t = \frac{2\Delta H - \frac{1}{2} M_c \omega^2 \xi(\frac{l}{2})}{mgl\omega^2} \sin \omega t \tag{5a}$$

and with hindering of the movement ($\gamma = o$) we have

$$\left.\begin{aligned} A_{(o)} + 2\Delta H - \tfrac{1}{2} M_c \omega^2 \xi(\tfrac{l}{2}) &= 0 \\ A_{(o)} &= 2K_1 \xi(\tfrac{l}{2}) \end{aligned}\right\} \tag{5b}$$

The A forces will be:

$$\left.\begin{aligned} A_1 = A\sin\omega t &= -\left(2\Delta H - \tfrac{1}{2} M_c \omega^2 \xi(\tfrac{l}{2})\right)\frac{x}{l}\sin\omega t \quad ; && 0 \le x \le \tfrac{l}{2} \\ A_1 = A\sin\omega t &= +\left(2\Delta H - \tfrac{1}{2} M_c \omega^2 \xi(\tfrac{l}{2})\right)\left(1-\frac{x}{l}\right)\sin\omega t \quad ; && \tfrac{l}{2} \le x \le l \end{aligned}\right\} \tag{6a}$$

and

$$\left.\begin{aligned} A_1 = A\sin\omega t &= -\left(2\Delta H - \tfrac{1}{2} M_c \omega^2 \xi(\tfrac{l}{2})\right)\sin\omega t \quad ; && 0 \le x \le \tfrac{l}{2} \\ A_1 = A\sin\omega t &= 0 && \tfrac{l}{2} \le x \le l \end{aligned}\right\} \tag{6b}$$

for the two types respectively.

As the bridges with some longitudinal movement are the most common, the deductions further on will be given for this type, and only the end results will be given for both types.

Equation (1. 7) may be written

$$\left.\begin{aligned} &JE\eta_1'''' - (H_{st} + \Delta H_1)y'' + H_1 \frac{\partial}{\partial x}(\eta_1' \sec^2\varphi) + \left(2\Delta H_1 - \tfrac{1}{2} M_c \omega^2 \xi_1(\tfrac{l}{2})\right)\frac{x}{l}(v''+\eta_1'') \\ &\quad + \left(2\Delta H_1 - \tfrac{1}{2} M_c \omega^2 \xi_1(\tfrac{l}{2})\right)\frac{1}{l}(v'+\eta_1') + m(x)\ddot{\eta}_1 = 0 \quad ; \qquad 0 \le x \le \tfrac{l}{2} \\ \text{and} \\ &JE\eta_1'''' - (H_{st} - \Delta H_1)y'' - H_1 \frac{\partial}{\partial x}(\eta_1' \sec^2\varphi) + \left(2\Delta H_1 - \tfrac{1}{2} M_c \omega^2 \xi_1(\tfrac{l}{2})\right)\left(\frac{x}{l}-1\right)(v''+\eta_1'') \\ &\quad + \left(2\Delta H_1 - \tfrac{1}{2} M_c \omega^2 \xi_1(\tfrac{l}{2})\right)\frac{1}{l}(v'+\eta_1') + m(x)\ddot{\eta}_1 = 0 \quad ; \qquad \tfrac{l}{2} \le x \le l \end{aligned}\right\} \tag{7}$$

Equations (11) and (12) give

$$(H_{st}+\Delta H_t)\frac{c\int_0^{\frac{l}{2}}\sec^3\varphi\,dx}{E_c A_c}+y''\int_0^{\frac{l}{2}}\eta_t\,dx=\xi_t\left(\tfrac{l}{2}\right)$$

$$(H_{st}-\Delta H_t)\frac{\int_{\frac{l}{2}}^{c'}\sec^3\varphi\,dx}{E_c A_c}+y''\int_{\frac{l}{2}}^{l}\eta_t\,dx=-\xi_t\left(\tfrac{l}{2}\right)$$

or

$$\left.\begin{aligned} H_{st}\frac{L_s}{E_c A_c}+y''\int_0^{l}\eta_t\,dx&=0\\ \Delta H_t\frac{L_s}{E_c A_c}+y''\left(\int_0^{\frac{l}{2}}\eta_t\,dx-\int_{\frac{l}{2}}^{l}\eta_t\,dx\right)&=2\xi_t\left(\tfrac{l}{2}\right)\end{aligned}\right\}\quad(8)$$

where $L_s=\int_c^{c'}\sec^3\varphi\,dx$

If the side cables are nonsymetric it will be an insignificant error in the last equation.

The deflection is introduced as

$$\eta_t=\eta\sin\omega t \qquad \text{and} \qquad \eta=\sum a_n\cdot\sin n\pi\frac{x}{l} \qquad (9)$$

Further we have

$$\xi_t=\xi\sin\omega t \quad ; \quad \gamma_t=\gamma\sin\omega t$$

$$H_{st}=H_s\sin\omega t \quad ; \quad \Delta H_t=\Delta H\sin\omega t$$

and

$$H_t=H_w+H_s\sin\omega t\pm\Delta H\sin\omega t$$

$$A_t=A\sin\omega t$$

In Equation (7) we introduce the approximation $\frac{\partial}{\partial x}(\eta'\sec^2\varphi)\approx\eta''\sec^2\varphi_m$ where φ_m is the mean value of the cable slope.

Consequently we write: $H_w\frac{\partial}{\partial x}(\eta'\sec^2\varphi)\approx H_w\sec^2\varphi_m\cdot\eta''=\bar{H}_w\cdot\eta''$

Equation (7) may be written

$$\left.\begin{aligned} &EJ\eta'''' - (H_s+\Delta H)y'' - (H_w + H_s\sin\omega t + \Delta H\sin\omega t)\frac{\partial}{\partial x}(\eta'\sec^2\varphi) \\ &+\left(2\Delta H - \tfrac{1}{2}M_c\omega^2\xi(\tfrac{l}{2})\right)\left(\tfrac{x}{l}(v''+\eta''\sin\omega t) + \tfrac{1}{l}(v'+\eta'\sin\omega t)\right) - \omega^2 m(x)\cdot\eta = 0 \\ &\qquad\qquad 0 \le x \le \tfrac{l}{2} \\ &\text{and} \\ &EJ\eta'''' - (H_s-\Delta H)y'' - (H_w + H_s\sin\omega t - \Delta H\sin\omega t)\frac{\partial}{\partial x}(\eta'\sec^2\varphi) \\ &+\left(2\Delta H - \tfrac{1}{2}M_c\omega^2\xi(\tfrac{l}{2})\right)\left(\left(\tfrac{x}{l}-1\right)(v''+\eta''\sin\omega t) + \tfrac{1}{l}(v'+\eta'\sin\omega t)\right) - \omega^2 m(x)\cdot\eta = 0 \\ &\qquad\qquad \tfrac{l}{2} \le x \le l \end{aligned}\right\} \quad (7a)$$

Introducing the approximation for $\sec^2\varphi$ and integrating the equations from o-T we obtain

$$\left.\begin{aligned} &EJ\eta''' - (H_s+\Delta H)y' - \bar{H}_w\cdot\eta'' + \left(2\Delta H - \tfrac{1}{2}M_c\omega^2\xi(\tfrac{l}{2})\right)\left(\tfrac{x}{l}v'' + \tfrac{1}{l}v'\right) - \omega^2 m(x)\cdot\eta = 0 \\ &\qquad\qquad 0 \le x \le \tfrac{l}{2} \\ &\text{and} \\ &EJ\eta''' - (H_s-\Delta H)y' - \bar{H}_w\cdot\eta'' + \left(2\Delta H - \tfrac{1}{2}M_c\omega^2\xi(\tfrac{l}{2})\right)\left(\left(\tfrac{x}{l}-1\right)v'' + \tfrac{1}{l}v'\right) - \omega^2 m(x)\eta = 0 \\ &\qquad\qquad \tfrac{l}{2} \le x \le l \end{aligned}\right\} \quad (7b)$$

In Eq. (7b) we introduce $\eta = \sum a_n \sin n\pi\frac{x}{l}$. Multiply each term with $\sin r\pi\frac{x}{l}$ and integrate over the span length o - l. This gives

$$\begin{aligned} &EJ\frac{\pi^4}{l^4}r^4 a_r \frac{l}{2} + \bar{H}_w\frac{\pi^2}{l^2}a_r\frac{l}{2} + H_s y''\frac{l}{\pi r}\left((-1)^r-1\right) - \Delta H y''\frac{l}{\pi r}\left(1+(-1)^r\right)\left(1-(-1)^{\frac{r}{2}}\right) \\ &-\left(\Delta H - \tfrac{1}{4}M_c\omega^2\xi(\tfrac{l}{2})\right)v''\frac{l}{\pi r}\left(1+(-1)^r\right)\left(1-(-1)^{\frac{r}{2}}\right) - m\omega^2\frac{l}{2}a_r = 0 \end{aligned} \quad (10)$$

where $y'' = -\frac{8f}{l^2}$; $v'' = -\frac{8vm}{l^2}$

H_s and ΔH are with use of Eq. (8), (9)

$$H_s = -\frac{E_c A_c}{L_s}y''\int_0^l \eta\,dx = \frac{E_c A_c}{L_s}\frac{32f}{\pi l}\sum\frac{a_n}{4n}\left(1-(-1)^n\right) \quad (8a)$$

$$\Delta H = \frac{E_c A_c}{L_s}\left\{2\xi\left(\tfrac{l}{2}\right) - y''\left(\int_0^{\frac{l}{2}} \eta\,dx - \int_{\frac{l}{2}}^{l} \eta\,dx\right)\right\} = \frac{E_c A_c}{L_s}\left(2\xi\left(\tfrac{l}{2}\right) + \frac{32f}{\pi l}\sum \frac{a_n}{4n}\left(1+(-1)^n\right)\left(1-(-1)^{\frac{n}{2}}\right)\right) \tag{9a}$$

The longitudinal movement $\xi\left(\frac{l}{2}\right)$ is given by the expression (3), and y'' is given by (5a) for a bridge with a longitudinal moving of the roadway.

The equations give

$$\xi\left(\tfrac{l}{2}\right) = \frac{\frac{2K_2}{m_g l\omega^2} - 1}{K_1 + \frac{1}{4}M_c\omega^2\left(\frac{2K_2}{m_g l\omega^2} - 1\right)}\,\Delta H = \vartheta\,\Delta H \tag{11}$$

This expression introduced in (9a) give

$$\Delta H = \varepsilon \sum \frac{a_n}{4n}\left(1+(-1)^n\right)\left(1-(-1)^{\frac{n}{2}}\right) \tag{12}$$

where

$$\varepsilon = \frac{32f}{\pi l\left(\frac{L_s}{E_c A_c} - 2\vartheta\right)}$$

ϑ and ε being functions of ω.

If the longitudinal movement of the bridge deck is hindered, we introduce $m_g l = \infty$ in the formulae (11) and (12).

Introducing H_s, ΔH and $\xi\left(\frac{l}{2}\right)$, Eq.'s (11) and (12), in Eq. (10)

$$\left.\begin{aligned}&\left\{\omega^2 - \alpha r^4 - \beta r^2\right\} a_r - \frac{1}{\lambda}\sum \frac{a_n}{4n}\left(1-(-1)^n\right)\left(1-(-1)^r\right)\\ &-\frac{1}{\chi}\left(1+\frac{\nu_{cm}}{f}\left(1-\frac{1}{4}M_c\vartheta\omega^2\right)\right)\sum \frac{a_n}{16\,r\,n}\left(1+(-1)^n\right)\left(1-(-1)^{\frac{n}{2}}\right)\left(1+(-1)^r\right)\left(1-(-1)^{\frac{r}{2}}\right) = 0\end{aligned}\right\} \tag{13}$$

where

$$\left.\begin{aligned}&\alpha = \frac{\pi^4 JE}{ml^4}\;;\quad \beta = \frac{\pi^2 H_w}{ml^2}\;;\quad \lambda = \frac{\pi^2 l^3}{8^3 f^2}\,\frac{m L_s}{E_c A_c}\;;\\ &\chi = \frac{\pi l^2 m}{8^2 f\varepsilon}\;;\quad \varepsilon = \frac{32f}{\pi l\left(\frac{L_s}{E_c A_c} - 2\vartheta\right)}\;;\quad \vartheta = \frac{1}{K_1\frac{m_g l\omega^2}{2K_2 - m_g l\omega^2} + \frac{1}{4}M_c\omega^2}\end{aligned}\right\} \tag{14}$$

If the longitudinal movement of roadway is hindered by the bearings in one end of the bridge, ϑ will be $\vartheta = \frac{1}{\frac{1}{4}M_c\omega^2 - K_1}$ the other expressions will be unchanged.

In studying Eq. (13) we divide the oscillations in symmetric- and antimetric-oscillations.

2.1.1. Symmetric oscillations.

$$\eta = \sum a_n \sin n\pi \frac{x}{l} \quad \text{where} \quad n = 1, 3, 5, 7, \ldots\ldots$$

Introducing this in Eq. (13) we get

$$\{\omega^2 - \alpha r^4 - \beta r^2\} a_r - \frac{1}{\lambda} \sum \frac{a_n}{4rn} \left(1-(-1)^{n}\right)\left(1-(-1)^{r}\right) = 0$$

$n = 1, 3, 5, \ldots\ldots$
$r = 1, 3, 5, \ldots\ldots$

or

$$\{\omega^2 - \alpha r^4 - \beta r^2\} a_r - \frac{1}{\lambda} \sum \frac{a_n}{rn} = 0 \qquad (15)$$

It is easily seen that by expressing the terms a_n in the series

$$\eta = \sum a_n \sin n\pi \frac{x}{l} \quad \text{by} \quad a_n = \frac{a_0}{n(\omega^2 - \alpha n^4 - \beta n^2)} \qquad (15a)$$

Equation (15) may be written

$$a_0 \frac{1}{r} - a_0 \frac{1}{\lambda} \sum \frac{1}{rn^2\{\omega^2 - \alpha n^4 - \beta n^2\}} = 0$$

or

$$\sum \frac{1}{n^2\{\omega^2 - \alpha n^4 - \beta n^2\}} = \lambda \quad ; \; n = 1, 3, 5, \ldots\ldots \qquad (16)$$

Solutions $a \gtrless 0$ mean that the denominator determinant in Eq. (15) must be Zero.

2.1.2. Antimetric oscillations.

Oscillations with 4-8-12-16 half waves, e.g. n=4-8-12-.

Equation (13) is reduced to

$$\{\omega^2 - \alpha r^4 - \beta r^2\} a_r = 0$$

or

$$\omega = r\sqrt{\alpha r^2 + \beta} \quad ; \; r = 4, (6), 8, (10), 12, \ldots\ldots \qquad (17)$$

The oscillation is represented by a single sine wave.

$$\eta = a_r \sin r\pi \frac{x}{l} \quad ; \quad r = 4, \ldots\ldots$$

Oscillations with 2, 6, 10,... half waves.

Introducing n= 2, 6, 10, ... and r= 2, 6 ...., in Equation (13) gives:

$$\{\omega^2 - \alpha r^4 - \beta r^2\} a_r - \frac{1}{\chi} \left\{1 + \frac{\nu m}{f}\left(1 - \tfrac{1}{4} M_c^2 \omega^2\right)\right\} \sum \frac{a_n}{rn} = 0$$

Introducing as before $a_n = \dfrac{a_0}{n\{\omega^2 - \alpha n^4 - \beta n^2\}}$ we get

$$\sum \frac{1}{n^2\{\omega^2 - \alpha n^4 - \beta n^2\}} = \frac{\chi}{1 + \frac{\nu m}{f}\left(1 - \frac{1}{4} M_c^2 \omega^2\right)} \; , \; n = 2, 6, 10, \ldots \qquad (18)$$

Where $\mathcal{L}$, and $\mathcal{V}$ are functions of ω see Eq. (13).

However this will not give any special trouble by the solution. Usually the most convenient will be to calculate the left and right hand side of Eq. (18) for distinct values of ω, and then find the points of intersection in a diagram. Important is however that Eq. (18) gives 2 different types of oscillation in 2 half waves, see Fig. 5. The two types are easy to demostrate on a model or a small bridge. As will be seen from Fig. 5, the results obtained by Eq. (18) are very good. If the longitudinal movement of the stiffening truss is hindered, there will be only one type of oscillation, however, the effect of the hanger inclination will still be important.

The effect of a vertical curvature of the stiffening truss will be small for all normal bridges as $\frac{v_m}{f}$ will be small.

If the suspender at midspan is Zero, $h(\frac{l}{2}) = 0$, the formulae will still be valid. Eq. (1, 14) give $K_1 = \infty$; $K_2 = \infty$; $\frac{K_1}{K_2} = 1$ which must be introduced in Eq. (9) - (18). Equation (18) give two values of ω_2, however, one will be without practical interest, see Fig. 5.

The value of ω for 6 or 10 half waves obtained from Eq. (18) will be almost identical to the value given by Eq. (17), and there is no reason for using Eq. (18) for those frequencies. In calculating ω_2 from Eq. (18) it will usually be sufficient to use one or two terms.

2. 2. Oscillations in a symmetrical three span suspension bridge.

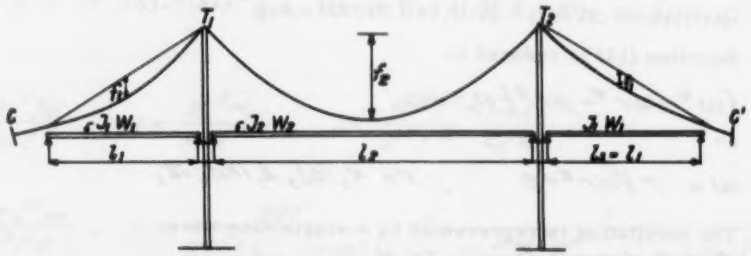

This type of bridges, see Fig. 9, are frequently built, and are of special interest to the designer.

The inclination of the hangers are of importance only in the main span, as the longitudinal movements in the side spans are small in the end where the hangers are short. Further, we suppose that the bearings at the towers don't hinder any longitudinal movement of the main span truss.

The oscillations are given by

$$\left.\begin{aligned} \eta_{1T} &= \eta_1 \sin \omega t \quad ; \quad \eta_1 = \Sigma a_{1n} \sin n\pi \frac{x}{l_1} \\ \eta_{2T} &= \eta_2 \sin \omega t \quad ; \quad \eta_2 = \Sigma a_{2n} \sin n\pi \frac{x}{l_2} \\ \eta_{3T} &= \eta_3 \sin \omega t \quad ; \quad \eta_3 = \Sigma a_{3n} \sin \pi \frac{x}{l_3} \end{aligned}\right\} \quad (19)$$

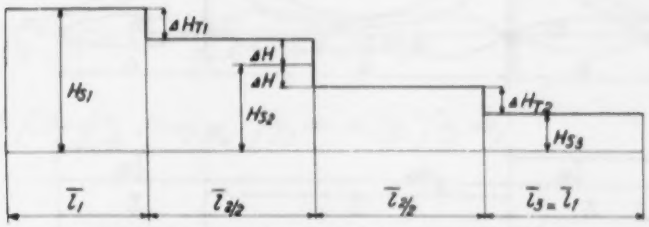

Fig. 10. Simplified variation of cable force.

The cable force will vary as indicated in Fig. 10. For symmetric and antimetric oscillations the variation is given in Fig. 11 and 12 respectively. For each separate span we have an equation analogous to Eq. (10) and (13).

$$\alpha_1 r_1^4 a_{1r} + \beta_1 r_1^2 a_{1r} + H_{S1} \frac{16 f_1}{m_1 l_1^2 \pi r_1} \left(1-(-1)^r\right) - \omega^2 a_{1r} = 0 \quad (20a)$$

$$\alpha_2 r_2^4 a_{2r} + \beta_2 r_2^2 a_{2r} + H_{S2} \frac{16 f_2}{m_2 l_2^2 \pi r_2} \left(1-(-1)^r\right)$$
$$+ \left\{\Delta H\left(1+\frac{\nu_2}{r_2}\right) - \frac{1}{4} M_c \omega^2 \xi\left(\frac{l}{2}\right)\frac{\nu_2}{r_2}\right\} \frac{16 f_2}{m_2 l_2^2 \pi r_2} \left(1+(-1)^r\right)\left(1-(-1)^{\frac{r}{2}}\right) - \omega^2 a_{2r} = 0 \quad (20b)$$

$$\alpha_1 r_3^4 a_{3r} + \beta_1 r_3^2 a_{3r} + H_{S3} \frac{16 f_1}{m_1 l_1^2 \pi r_3} \left(1-(-1)^r\right) - \omega^2 a_{3r} = 0 \quad (20c)$$

As may readily be seen from Eq. (20) all oscillations which give $H_s = o$ and $\Delta H = o$ will be independent for each span. The frequencies are given by

$$\left.\begin{aligned} \omega_{1r} &= r_1 \sqrt{\alpha_1 r_1^2 + \beta_1} \quad ; r_1 = 2, 4, 6, \cdots \\ \omega_{2r} &= r_2 \sqrt{\alpha_2 r_2^2 + \beta_2} \quad ; r_2 = 4, (6), 8, \cdots \\ \omega_{3r} &= \omega_{1r} \end{aligned}\right\} \quad (21)$$

All other types of oscillations will be coupled. For oscillations with 6; 10; ... half waves in the main span the coupling will be small and Eq. (21) will be sufficiently correct.

2.2.1. Symmetrical oscillations. See Fig. 11.

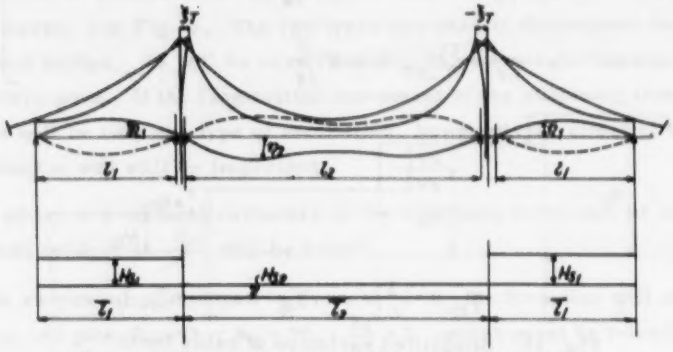

Fig. 11. Symmetric oscillation of a three span suspension bridge.

$$\eta_3 = \eta_1 \qquad a_{3n} = a_{1n}$$

In span 1 we have

$$H_{s1}\frac{L_{s1}}{E_c A_c} + y_1'' \int_0^{l} \eta_1\, dx = \xi(l) = \xi_p$$

and for span 2:

$$H_{s2}\frac{L_{s2}}{E_c A_c} + y_2'' \int \eta_2\, dx = -\xi(0) + \xi(l) = -2\xi_p \qquad (22)$$

where

$$L_{s1} = \int_{c_1}^{T_1} \sec^3\varphi\, dx \quad ; \quad L_{s2} = \int_{T_1}^{T_2} \sec^3\varphi\, dx$$

Between H_{s1}; H_{s2} and ξ_p we have the following relation. The oscillating tower system is replaced by a spring S_p and a consentrated mass M_p giving the same resistance against any static deflection of tower and having the same circular frequency ω_p as the tower.

$$S_p = \omega_p^2 M_p \qquad (23)$$

S_p and ω_p are values given by the tower construction. When calculating ω_p we have to remember that the cable masses $\approx \frac{1}{2}M_{c1}$ and $\approx \frac{1}{4}M_{c2}$ follow the tower.

We have

$$-(H_{s1}-H_{s2}) = S_p \xi_p - \omega^2 M_p \xi_p$$

$$\xi_p = -\frac{H_{s1}-H_{s2}}{S_p-\omega^2 M_p} = -\frac{H_{s1}-H_{s2}}{S_p\left(1-\left(\frac{\omega}{\omega_p}\right)^2\right)} = -\frac{1}{F(\omega)}(H_{s1}-H_{s2}) \qquad (24)$$

Introducing ξ_p in Eq. (22) we get

$$\left.\begin{aligned} H_{s1} &= -\frac{1}{D_s}\left(y_2''\int\eta_2\,dx + \left(2+\frac{L_{s2}}{E_c A_c}F(\omega)\right)y_1''\int\eta_1\,dx\right) \\ H_{s2} &= -\frac{1}{D_s}\left(\left(1+\frac{L_{s1}}{E_c A_c}F(\omega)\right)y_2''\int\eta_2\,dx + 2y_1''\int\eta_1\,dx\right) \end{aligned}\right\} \qquad (25)$$

where

$$D_s = \frac{L_{s2}+2L_{s1}}{E_c A_c} + \frac{L_{s2}\cdot L_{s1}}{E_c^2\cdot A_c^2}\cdot F(\omega)$$

and

$$y_2''\int_0^l \eta_2\,dx = -\frac{32 f_2}{\pi l_2}\sum\frac{a_{2n}}{4n_2}\left(1-(-1)^n\right);\quad n=1,3,5,\ldots\ldots$$

$$y_1''\int_0^l \eta_1\,dx = -\frac{32 f_1}{\pi l_1}\sum\frac{a_{1n}}{4n_1}\left(1-(-1)^n\right);\quad n=1,3,5,\ldots\ldots$$

Introducing H_{s1}; H_{s2} in Eq. (20) we obtain

$$\left.\begin{aligned} &\left\{\omega^2-\alpha_1 r_1^4-\beta_1 r_1^2\right\}a_{1r} - \frac{1}{\lambda_1}\frac{L_{s1}}{E_c A_c}\frac{\left(2+\frac{L_{s2}}{E_c A_c}F(\omega)\right)}{D_s}\sum\frac{a_{1n}}{r_1 n_1} - \frac{1}{\lambda_2}\frac{m_2 l_2^2 f_1}{m_1 l_1^2 f_2}\frac{L_{s2}}{A_c E_c}\frac{1}{D_s}\sum\frac{a_{2n}}{r_1 n_2} = 0 \\ &\left\{\omega^2-\alpha_2 r_2^4-\beta_2 r_2^2\right\}a_{2r} - \frac{1}{\lambda_2}\frac{L_{s2}}{E_c A_c}\frac{\left(1+\frac{L_{s1}}{E_c A_c}F(\omega)\right)}{D_s}\sum\frac{a_{2n}}{r_2 n_2} - \frac{1}{\lambda_1}\frac{m_1 l_1^2 f_2}{m_2 l_2^2 f_1}\frac{L_{s1}}{A_c E_c}\frac{2}{D_s}\sum\frac{a_{1n}}{r_2 n_1} = 0 \\ &\frac{1}{\lambda_1} = \frac{8^3 f_1^2}{\pi^2 l_1^2}\frac{E_c A_c}{m_1 L_{s1}};\quad \frac{1}{\lambda_2} = \frac{8^3 f_2^2}{\pi^2 l_2^2}\frac{E_c A_c}{m_2 L_{s2}};\quad L_s = 2L_{s1}+L_{s2} \end{aligned}\right\} \qquad (26)$$

A direct solution if Eq. (26) like Eq. (16) does not exist. However, as we usually only need a few terms in the series

$$\eta_1 = \sum a_1 \sin n\pi\frac{x}{l_1};\quad \eta_2 = \sum a_2 \sin n\pi\frac{x}{l_2}$$

to get a good result, the solving of Eq. (26) gives no difficulties. In fact it will usually be sufficient with 1 or 2 terms in the series for η_1, and 2 or 3 terms in the series for the main span. To get solutions $\eta_1 \gtrless 0$; $\eta_2 \gtrless 0$ we have that the denominator determinant $|D| = o$, which gives an equation for finding ω. With ω known, the relations between a_{11}; a_{13}; a_{21} etc. are readily found from Eq. (26).

Neglecting the stiffness and masses at the towers e. g. introducing $F(\omega) = S_p - \omega^2 M_p = o$, a direct solution may be found.

Introducing $F(\omega) = o$ and

$$a_{1n} = \frac{a_o}{n_1(\omega^2 - \alpha_1 n_1^4 - \beta_1 n_1^2)} \frac{f_1}{m_1 l_1^2}$$

$$a_{2n} = \frac{a_o}{n_2(\omega^2 - \alpha_2 n_2^4 - \beta_2 n_2^2)} \frac{f_2}{m_2 l_2^2}$$

into Eq. (26) gives

$$\frac{L_{s2}}{L_s} \frac{1}{\lambda_2} \sum_{1,3,5,\cdots} \frac{1}{n_2^2(\omega^2 - \alpha_2 n_2^4 - \beta_2 n_2^2)} + \frac{L_{s1}}{L_s} \frac{2}{\lambda_1} \sum_{1,3,5,\cdots} \frac{1}{n_1^2(\omega^2 - \alpha_1 n_1^4 - \beta_1 n_1^2)} - 1 = 0 \quad (27)$$

Usually it will be sufficient to handle just a few terms in the series. If $F(\omega) \lesssim 0$; Eq. (27) may be used for finding a first approximate solution of Eq. (26), usually the difference between results obtained from Eq. (26) and (27) will be small.

Generally we may write

$$\sum_m \frac{L_{sm}}{L_s} \frac{1}{\lambda_m} \sum_n \frac{1}{n_m^2(\omega^2 - \alpha_m n_m^4 - \beta_m n_m^2)} - 1 = 0 \quad (28)$$

for a m span bridge with $F(\omega) = o$ at all towers. However, true symmetrical oscillations are only possible if the bridge is symmetrical.

2. 2. 2. Antimetric oscillations. See Fig. 12.

The oscillation is given by $\eta_1 = \eta \sin \omega t$, where

$$\eta_1 = \sum a_{1n} \sin n\pi \frac{x}{l_1} \; ; \; n = 1, 3, 5, \cdots$$

$$\eta_2 = \sum a_{2n} \sin n\pi \frac{x}{l_2} \; ; \; n = 2, 6, 10, \cdots$$

$$\eta_3 = -\eta_1$$

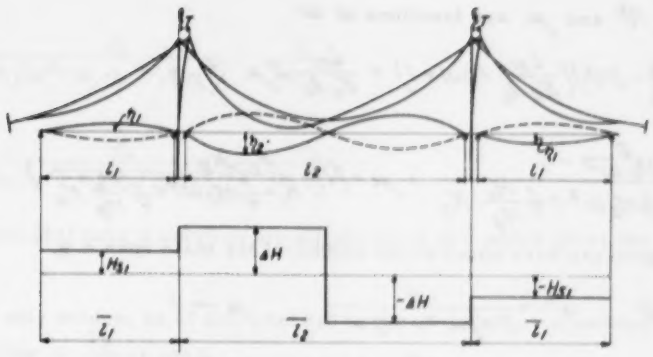

Fig. 12. Antimetric oscillation of a three span suspension bridge.

The cable force will be given by the Equations

$$H_{S2}=0 \quad ; \quad H_{S3}=-H_{S1}$$

$$H_{S1}\cdot\frac{L_{S1}}{E_c A_c}+y_1''\int\eta_1\,dx=\xi_p \qquad (8)$$

$$\Delta H=+\frac{1}{4}M_c\omega^2\xi\left(\frac{l}{2}\right)-K_1\xi\left(\frac{l}{2}\right)+K_2\gamma+(K_1-K_2)\xi_p \qquad (3)$$

$$2\Delta H-\frac{1}{2}M_c\omega^2\xi\left(\frac{l}{2}\right)=\gamma m_{g_2} l_2\omega^2=\gamma M_{g_2}\omega^2 \qquad (5a)$$

$$\Delta H\frac{L_{S2}}{E_c A_c}+y_2''\left(\int_0^{\frac{l}{2}}\eta_2\,dx-\int_{\frac{l}{2}}^{l}\eta_2\,dx\right)=2\xi\left(\frac{l}{2}\right)-2\xi_p \qquad (8)$$

The movement of the towers are given by

$$\xi_p=-\frac{H_{S1}-\Delta H}{S_p-\omega^2 M_p}=-\frac{1}{F(\omega)}\,(H_{S1}-\Delta H) \qquad (29)$$

By elimination we get

$$H_{S1}=-\frac{1}{D_a}\left\{\left[\left(\frac{L_{S2}}{E_c A_c}-2\nu\right)F(\omega+2\mu\right]y_1''\int_0^{l}\eta_1\,dx+y_2''\left(\int_0^{\frac{l}{2}}\eta_2\,dx-\int_{\frac{l}{2}}^{l}\eta_2\,dx\right)\right\}$$

$$\Delta H=-\frac{1}{D_a}\left\{\left(\frac{L_{S1}}{E_c A_c}F(\omega)+1\right)y_2''\left(\int_0^{\frac{l}{2}}\eta_2\,dx-\int_{\frac{l}{2}}^{l}\eta_2\,dx\right)+2\mu y_1''\int_0^{l}\eta_1\,dx\right\} \qquad (30)$$

$$\xi\left(\frac{l}{2}\right)=\left(\nu+\frac{1-\mu}{F(\omega)}\right)\Delta H-\frac{1-\mu}{F(\omega)}H_{S1}$$

where D_a, ν and μ are functions of ω

$$D_a = \left(\frac{L_{s2}}{E_c A_c} - 2\nu\right)\left(\frac{L_{s1}}{E_c A_c} F(\omega) + 1\right) + \frac{L_{s1}}{E_c A_c} 2\mu$$

$$\nu = \frac{K_2 \frac{2}{M_g}\omega^2 - 1}{K_1 - \frac{1}{4} M_c \omega^2 + \frac{1}{2}\frac{M_c}{M_g} K_2} \quad ; \quad \mu = \left(1 - \frac{K_1 - K_2}{K_1 - \frac{1}{4} M_c \omega^2 + \frac{1}{2}\frac{M_c}{M_g} K_2}\right) \qquad (31)$$

If the hangers are very short at the middle of the main span e. g.

$$h\left(\frac{l}{2}\right) \to 0 \quad ; \quad \nu \to \frac{4}{2 M_g \omega^2 + M_c \omega^2} \quad ; \quad \mu \to 1$$

If the hanger $h\left(\frac{l}{2}\right)$ increases ν and μ have the limit

$$\nu \to \frac{4}{M_c \omega^2} \quad ; \quad \mu \to 1 \quad ; \quad h\left(\frac{l}{2}\right) \to \infty$$

Usually ν, μ will be near the values at the first limit

$$y_1'' \int_0^l \eta_1 dx = -\frac{32 f_1}{\pi l_1} \sum \frac{a_1 n_1}{4 n_1} \left(1 - (-1)^{n}\right) \quad ; \quad n_1 = 1, 3, 5, \cdots\cdots$$

$$y_2''\left(\int_0^{\frac{l}{2}} \eta_2 dx - \int_{\frac{l}{2}}^{l} \eta_2 dx\right) = -\frac{32 f_2}{\pi l_2} \sum \frac{a_2 n_2}{4 n_2} \left(1 + (-1)^{n}\right)\left(1 - (-1)^{\frac{n}{2}}\right) \quad ; \quad n = 2, 6, 10, \cdots$$

Neglecting $\frac{\omega^2}{f_2}$ and introducing H_{s1} and ΔH in Eq. (20) results in:

$$\begin{aligned}
&a_1\left\{1 - \frac{1}{\lambda_1}\left(\left(\frac{L_{s2}}{E_c A_c} - 2\nu\right) F(\omega) + 2\mu\right)\frac{L_{s1}}{E_c A_c D_a} \sum_{1,3,5} \frac{1}{n^2\{\omega^2 - \alpha_1 n^4 - \beta_1 n^2\}}\right\} \\
&- a_2 \frac{1}{2\chi_2} \frac{\frac{L_{s2}}{E_c A_c} - 2\nu}{D_a} \sum_{2,6,10} \frac{1}{n^2\{\omega^2 - \alpha_2 n^4 - \beta_2 n^2\}} = 0 \\
&a_2\left\{1 - \frac{1}{\chi_2} \frac{\left(\frac{L_{s2}}{E_c A_c} - 2\nu\right)\left(\frac{L_{s1}}{E_c A_c} F(\omega) + 1\right)}{D_a} \sum_{2,6,10} \frac{1}{n^2\{\omega^2 - \alpha_2 n^4 - \beta_2 n^2\}}\right\} \\
&- a_1 \frac{2}{\lambda_1} \frac{L_{s1}}{E_c A_c} \frac{2\mu}{D_a} \sum_{1,3,5} \frac{1}{n_1^2\{\omega^2 - \alpha_1 n^4 - \beta_1 n^2\}} = 0
\end{aligned} \qquad (32)$$

where

$$\frac{1}{\lambda_1} = \frac{8^3 f_1^2}{\pi^2 l_1^3 m_1} \frac{E_c A_c}{L_{s1}} \quad ; \quad \frac{1}{\chi_2} = \frac{4 \cdot 8^3 f_2^2}{\pi^2 l_2^3 m_2 \left(\frac{L_{s2}}{E_c A_c} - 2\nu\right)}$$

and

$$a_{1n} = \frac{a_1}{n_1\{\omega^2 - \alpha_1 n_1^4 - \beta_1 n_1^2\}} \cdot \frac{f_1}{m_1 l_1^2}$$

$$a_{2n} = \frac{a_2}{n_2\{\omega^2 - \alpha_2 n_2^4 - \beta_2 n_2^2\}} \cdot \frac{f_2}{m_2 l_2^2} \qquad (33)$$

Equation (32) have a solution for all values of ω^2 which gives the Denominator D = 0.

It will only seldom be of any interest to use more exact equations where the true value of $\frac{V_2}{f_2}$ is used.

2.3. Oscillations in a two span suspension bridge.

Sometimes a bridge of this type will be built. The inclination of the hangers will be of importance only in the main span. We further assume that the longitudinal movement of the main span truss will not be hindered.

The oscillations are given by

$$\eta_{1t} = \eta_1 \sin \omega t \quad ; \quad \eta_1 = \sum a_{1n} \sin n\pi \frac{x}{l_1}$$

$$\eta_{2t} = \eta_2 \sin \omega t \quad ; \quad \eta_2 = \sum a_{2n} \sin n\pi \frac{x}{l_2} \qquad (34)$$

The cable force will vary as indicated in Fig. 13.

For span 1 and 2 respectively we have the Equations (20a) and (20b).

An oscillation giving $H_s = 0$; $\Delta H = 0$ is independent for the two spans and will be as given in Eq. (21). All other oscillations will be coupled. For oscillations with 6, 10, half waves dominating in the main span the coupling effect will be negligible and Eq. (21) may be used.

Of technical interest will be when 1 wave dominate in span 1, and 1; 2 or 3 dominate in span 2. Usually there is no reason for using more than one term a_{11} in the series for η_1; the terms a_{21}, a_{22} when investigating one or two half waves in the main span and a_{21}, a_{22} and a_{23} when eventually investigating oscillations with 3 half waves. See Fig. 13.

The cable forces, and movement of tower, cable and truss are given by the equations:

$$H_{s1} \frac{L_{s1}}{E_c A_c} + y_1'' \int_0^l \eta_1 \, dx = \xi p \qquad (8)$$

$$H_{s2} \frac{L_{s2}}{E_c A_c} + y_2'' \int_0^l \eta_2 \, dx = -\xi p \qquad (8)$$

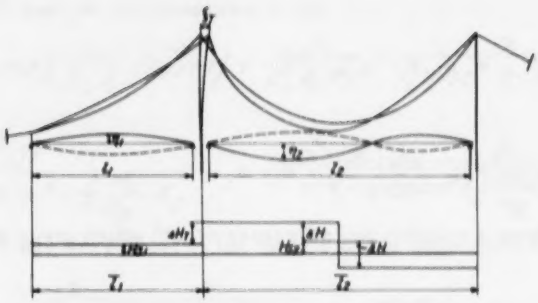

Fig. 13. Oscillation of two span suspension bridge.

$$\Delta H \frac{L_{s2}}{E_c A_c} + y_2'' \left[\int_0^{\frac{l}{2}} \eta_2 \, dx - \int_{\frac{l}{2}}^{l} \eta_2 \, dx \right] = 2 \xi_2 \left(\tfrac{l}{2}\right) - \xi_p \tag{8}$$

$$\Delta H = \omega^2 M_c \tfrac{1}{4} \xi_2 \left(\tfrac{l}{2}\right) - K_1 \xi_2 \left(\tfrac{l}{2}\right) + K_2 y_2 + \tfrac{1}{2}(K_1 - K_2) \xi_p \tag{3}$$

$$2\Delta H - \tfrac{1}{2} M_c \omega^2 \xi_2 \left(\tfrac{l}{2}\right) = y_2 \, m_{g_2} \, l_2 \, \omega^2 \tag{5}$$

$$\xi_p = - \frac{H_{s1} - H_{s2} - \Delta H}{S_p - \omega^2 M_p} = \frac{1}{F(\omega)} (H_{s1} - H_{s2} - \Delta H) \tag{29}$$

By elimination we get all the necessary data.

Neglecting $\frac{y_2}{l_2}$ we get the following 3 equations:

$$a_1 \left\{ 1 - \frac{1}{\lambda_1} L_{s1} \frac{\left(\frac{L_{s2}}{E_c A_c} - 2\vartheta\right)\left(\frac{L_{s2}}{E_c A_c} F(\omega) + 1\right) + (1-\mu)\frac{L_{s2}}{E_c A_c}}{E_c A_c \, D} \sum_{1,3,} \frac{1}{n_1^2 \{\omega^2 - \alpha_1 n_1^4 - \beta_1 n_1^2\}} \right\}$$

$$- a_s \frac{1}{\lambda_2} \frac{L_{s2}\left(\frac{L_{s2}}{E_c A_c} - 2\vartheta\right)}{E_c A_c \, D} \sum_{1,3,5,} \frac{1}{n^2 \{\omega^2 - \alpha_2 n^4 - \beta_2 n^2\}}$$

$$- a_a \frac{1}{2\lambda_2} \frac{L_{s2}\left(\frac{L_{s2}}{E_c A_c} - 2\vartheta\right)}{E_c A_c \, D} \sum_{2,6,} \frac{1}{n^2 \{\omega^2 - \alpha_2 n^4 - \beta_2 n^2\}} = 0 \tag{35a}$$

$$- a_1 \frac{1}{\lambda_1} L_{s1} \frac{\left(\frac{L_{s2}}{E_c A_c} - 2\vartheta\right)}{E_c A_c \, D} \sum_{1,3,} \frac{1}{n_1^2 \{\omega^2 - \alpha_1 n^4 - \beta_1 n^2\}}$$

$$+ a_s \left\{ 1 - \frac{1}{\lambda_2} L_{s2} \frac{\left(\frac{L_{s2}}{E_c A_c} - 2\vartheta\right)\left(\frac{L_{s1}}{E_c A_c} F(\omega) + 1\right) + (1-\mu)\frac{L_{s1}}{E_c A_c}}{E_c A_c \, D} \sum_{1,3,} \frac{1}{n^2 \{\omega^2 - \alpha_2 n^4 - \beta_2 n^2\}} \right\}$$

$$+ a_a \frac{1}{2\lambda_2} L_{s1} \frac{\left(\frac{L_{s2}}{E_c A_c} - 2\vartheta\right)}{E_c A_c \, D} \sum_{2,6,} \frac{1}{n^2 \{\omega^2 - \alpha_2 n^4 - \beta_2 n^2\}} = 0 \tag{35b}$$

$$-a_1\frac{1}{\lambda_1}L_{s1}\frac{(1-\mu)\frac{L_{s2}}{E_cA_c}}{E_cA_c\ D}\sum_{1,3,}\frac{1}{n^2\{\omega^2-\alpha_1 n^4-\beta_1 n^2\}}$$

$$+a_3\frac{2}{\lambda_2}L_{s2}\frac{(1-\mu)\frac{L_{s1}}{E_cA_c}}{E_cA_c\ D}\sum_{1,3,}\frac{1}{n^2\{\omega^2-\alpha_2 n^4-\beta_2 n^2\}} \qquad (35c)$$

$$+a_a\left\{1-\frac{1}{\lambda_2}\frac{\left(\frac{L_{s2}}{E_cA_c}-2\vartheta\right)\left(L_{s1}+L_{s2}+\frac{L_{s2}\cdot L_{s1}}{E_cA_c}\cdot F(\omega)\right)}{E_cA_c\ D}\sum_{2,6,}\frac{1}{n^2\{\omega^2-\alpha_2 n^4-\beta_2 n^2\}}\right\}=0$$

Where λ and $\varkappa$ are the same as given before, f. inst. in Eq. (33), ϑ and μ are given by Eq. (31) and D is given by

$$D=\left(\frac{L_{s2}}{E_cA_c}-2\vartheta\right)\left(\frac{L_{s1}}{E_cA_c}+\frac{L_{s2}}{E_cA_c}+\frac{L_{s1}\cdot L_{s2}}{E_c^2A_c^2}F(\omega)\right)+(1-\mu)\frac{L_{s1}L_{s2}}{E_c^2A_c^2} \qquad (36)$$

For the coefficients a_{1n}; a_{2n} are introduced

$$\left.\begin{aligned} a_{1n}&=\frac{a_1}{n\{\omega^2-\alpha_1 n^4-\beta_1 n^2\}}\frac{f_1}{m_1 l_1^2} \quad ; n=1,3,5,\cdots\cdots \\ a_{2n}&=\frac{a_3}{n\{\omega^2-\alpha_2 n^4-\beta_2 n^2\}}\frac{f_2}{m_2 l_2^2} \quad ; n=1,3,5,\cdots\cdots \\ a_{2n}&=\frac{a_a}{n\{\omega^2-\alpha_2 n^4-\beta_2 n^2\}}\frac{f_2}{m_2 l_2^2} \quad ; n=2,6,\cdots\cdots \end{aligned}\right\} \qquad (37)$$

The value of ω^2 which gives the denominator determinant of the Eq.'s (35) identical to Zero represents the solutions of equation (35) where oscillations can exsist.

For special cases f. inst. $h(\frac{1}{2})\to\infty$; $F(\omega)\to 0$ the equations (35) simplify to equations as given before, e. g. Eq. (16); (18) and (28).

Equations for oscillations in a 3 span bridge with different side spans may be deduced in the same manner. However, by substituting a mean value for the side spans a sufficiently correct solution will always be found.

3. NATURAL FREQUENCIES IN TORSIONAL OSCILLATIONS.

3.1. Deduction of Equations.

This type of oscillations may be investigated in the same manner as for vertical oscillations.

When oscillating in a free torsional oscillation the bridge will have a fixed axis of rotation, and we pressume that the angle of oscillation is small.

The torsion of an element is governed by the equation

$$M_p = \Sigma G I_D \frac{d\varphi_t}{dx} - \Sigma E C_w \frac{d^3\varphi_t}{dx^3} \qquad (1)$$

$\Sigma G\, I_D$ is the sum of torsional stiffness of the bridge section and $\Sigma E\, C_w$ is the sum of warping resistance of the section. Formulae for I_D and C_w is given in chapt. 3.2.

φ_t is the angle of rotation. As we assume this angle to be small we introduce $\tan\varphi \approx \varphi$; $\cos \approx 1$.

The mass of the bridge section and the weight of the section will resist the torsion with a moment

$$M(x,t) = \int_m (r^2 dm) \frac{d^2\varphi_t}{dt^2} + 2S(h_r - h_w)\,\varphi_t \qquad (2)$$

where m is the mass, r the distance from centre of rotation, S is the hanger force per linear length and per cable. h_r is the vertical distance between the fixing of hangers on the bridge section and the centre of rotation, and h_w is the distance between centre of gravity and centre of rotation. See also Fig. 14.

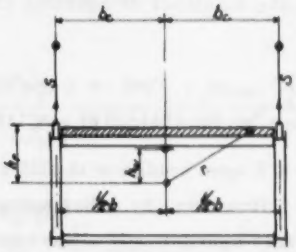

Fig. 14. Cross section of bridge.

We introduce

$$M = \int_m r^2 dm \qquad (3)$$

and replace the angle of rotation φ with the vertical movement of the cables.

$$\varphi_t = \frac{\eta_t}{b_c} \qquad (4)$$

Equation (1. 7) given for vertical oscillations will now read

$$\left.\begin{aligned}&(\Sigma EC_w)\frac{1}{b_c}\eta_t'''' - (H_{st}+\int dH)\,2b_c\,y'' - H_t 2b_c\,\frac{\partial}{\partial x}(\eta_t'\sec^2\varphi) - \Sigma GI_D\frac{1}{b_c}\eta_t''\\ &-H'2b_c y' - A_t 2\left(\frac{b}{2}v''+b_c\eta_t''\right) - A_t' 2\left(\frac{b}{2}v'+b_c\eta_t'\right) + M(x,t) = F(x,t)\end{aligned}\right\} \quad (5)$$

All previously deduced equations for H, A and ξ will be valid. $\gamma \equiv 0$, as we easily may see this is the only possible value of γ with pure torsional oscillations.

Equations (1. 7) and (3. 5) being of the same form conclude in an investigation along the same line.

Introducing

$$\eta_t = \eta \sin \omega_T t \;;\quad \omega_T = \frac{2\pi}{T} \qquad (6)$$

we may use all in chapter (2) derived formulae for calculating the natural torsional frequencies.

In the formulaes we replace

$$\omega^2 \quad \text{with} \quad \omega_T^2 - \frac{S(H_T + H_w)}{M} \qquad (7)$$

except where we have tower resistance where ω^2 is replaced by ω_T^2.

Consequently we introduce:

$$\alpha = \alpha_T = \frac{\pi^4 \Sigma C_w E}{l^4 M} \qquad (2.14) \qquad (8a)$$

$$\beta = \beta_T = \frac{\pi^2(\bar{H}_w 2b_c^2 + \Sigma GI_D)}{l^2 M} \qquad " \qquad (8b)$$

$$\frac{1}{\lambda} = \frac{1}{\lambda_T} = \frac{8^3 f^2 2b_c^2}{\pi^2 l^3 M}\,\frac{E_c A_c}{L_s} \qquad " \qquad (8c)$$

$$\varepsilon = \varepsilon_T = \frac{32 f}{\pi l\left(\frac{L_s}{E_c A_c} - 2\vartheta\right)} \qquad " \qquad (8d)$$

$$\frac{1}{\chi} = \frac{1}{\chi_T} = \frac{4\cdot 8^3 f^2 2b_c^2}{\pi^2 l^3 M}\,\frac{1}{\left(\frac{L_s}{E_c A_c} - 2\vartheta\right)} \qquad " \qquad (8e)$$

$$\vartheta = \vartheta_T = \frac{-1}{K_1 - \frac{1}{4}M_c\omega_T^2} \qquad (2.14)\quad (2.31) \qquad (8f)$$

$$\mu = \mu_T = \left(1 - \frac{K_1 - K_2}{K_1 - \frac{1}{4}M_c\omega_T^2}\right) \qquad " \qquad (8g)$$

$$F(\omega) = F(\omega_T) = S_p' - \omega_T^2 M_p' = S_p'\left(1 - \left(\frac{\omega_T}{\omega_p}\right)^2\right) \qquad (2.24) \qquad (8h)$$

Further we replace

$$\{\omega^2 - \alpha n^4 - \beta n^2\} \text{ by } \{\omega_T^2 - \frac{S(h_r - h_{ri})}{M} - \alpha_T n^4 - \beta_T n^2\} \tag{9}$$

With all this substitutions the formulae given in (2. 1), (2. 2), and (2. 3) may be used directly.

3. 2. Torsional stiffness and warping.

In this paper will be given an elementary deduction of the torsional stiffness and the warping resistance.

The cross-section consists of the chords A_1; A_2 and lattice systems between the chords as indicated in Fig. 15.

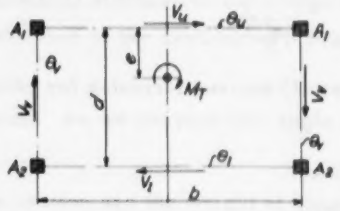

Fig. 15. Forces due to torsion.

The centre of rotation has a distance e from the upper lattice system. In Fig. 16 are shown the shear forces and axial forces in the system.

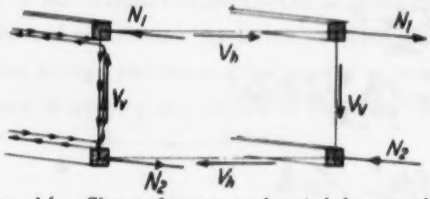

Fig. 16. Shear forces and axial forces due to torsion.

The deflection of a girder due to the shear deformation of the lattice system is given by:

$$\eta_v' = \frac{V}{G\Theta} \tag{10}$$

The total deformation η of a girder is separated in a part η_M due to the moment and a part η_v due to the shear.

$$\eta = \eta_M + \eta_V$$

A torsional moment M_T is acting on the section and produce shear forces in the trusses.

We have $V_u = V_l = V_h$ and $M_T = V_h \cdot d + V_v \cdot b$ (11)

Further, with small deformations the axial force in the chords will be

$N_1 = N_2 = N$.

The deflection is given by the angle of rotation φ and the rotation centre. The curvature of the girders will be:

$$\frac{1}{\rho} = \eta'' = \eta_V'' + \eta_M'' = 0\varphi''$$

Vertical girders:

$$\frac{1}{2}\varphi'' b = \frac{V_v'}{G\theta_v} + \frac{N}{Ed}\left(\frac{1}{A_1} + \frac{1}{A_2}\right) \tag{11a}$$

Upper horizontal girder:

$$\varphi'' e = \frac{V_h'}{G\theta_u} - \frac{N}{Eb}\frac{2}{A_1} \tag{11b}$$

Lower horizontal girder:

$$\varphi''(d-e) = \frac{V_h'}{G\theta_l} - \frac{N \cdot 2}{Eb \cdot A_2} \tag{11c}$$

Introducing

$$\frac{1}{\theta_h} = \frac{1}{2}\left(\frac{1}{\theta_u} + \frac{1}{\theta_l}\right) \tag{12}$$

The equations (11) yield

$$\varphi'' bd = \frac{V_v'}{G\theta_v} \cdot d + \frac{V_h'}{G\theta_h} \cdot b$$

or

$$\frac{d}{G\theta_v} V_v + \frac{b}{G\theta_h} V_h = \varphi' bd \tag{13}$$

The axial force is given by the shear forces

$$dN = -\frac{V_v}{d}dx + \frac{V_h}{b}dx$$

or

$$N' = -\frac{1}{d}V_v + \frac{1}{b}V_h \tag{14}$$

We now have a sufficient number of equations to express V_v; V_h and N by φ.

Introducing the notations

$$\xi = \frac{bd\theta_v\theta_h}{b^2\theta_v + d^2\theta_h} \quad ; \chi = \frac{db\xi}{\theta_v\theta_h} \cdot \frac{A_1 A_2}{(A_1 + A_2)} \tag{15}$$

we get

$$N' = -G\theta_v \frac{b}{d}\varphi' + \frac{\theta_v}{d\xi} V_h = +G\theta_h \frac{d}{b}\varphi' - \frac{\theta_h}{b\xi} V_v \tag{16}$$

$$V_v = Gd\xi\varphi' - E\tfrac{1}{2}b\theta_v\chi\varphi''' + \frac{E}{G}\chi V_v''$$
$$V_h = Gb\xi\varphi' - E\tfrac{1}{2}d\theta_h\chi\varphi''' + \frac{E}{G}\chi V_h'' \qquad (17)$$

Replacing V_v'' ; V_h'' by the double derivatives of Eq. (17) we get

$$V_v = Gd\xi\varphi' - E\chi(\tfrac{1}{2}b\theta_v - d\xi)\varphi''' - \frac{E^2}{G}\chi^2(\tfrac{1}{2}b\theta_v - d\xi)\varphi^{(5)} \cdots\cdots$$

$$V_h = Gb\xi\varphi' - E\chi(\tfrac{1}{2}d\theta_h - b\xi)\varphi''' - \frac{E^2}{G}\chi^2(\tfrac{1}{2}d\theta_h - b\xi)\varphi^{(5)} \cdots\cdots$$

Neglection of terms of higher derivatives than 3 is identical to the usual neglection of shear deformation of beams. Consequently

$$V_v = Gd\xi\varphi' - E\chi(\tfrac{1}{2}b\theta_v - d\xi)\varphi'''$$
$$V_h = Gb\xi\varphi' - E\chi(\tfrac{1}{2}d\theta_h - b\xi)\varphi''' \qquad (18)$$

Introduction of this result in Eq. (11) yields:

$$M_T = GI_D\varphi' - EC_w\varphi''' \qquad (19)$$

where

$$I_D = 2db\xi$$
$$C_w = \chi\frac{\theta_v\cdot\theta_h}{\xi}db\left(\frac{l}{2} - 2\frac{\xi^2}{\theta_v\theta_h}\right) = 2\frac{A_1\cdot A_2}{A_1+A_2}b^2d^2\left(\frac{l}{2} - \frac{d\xi}{b\theta_v}\right)^2 \qquad (20)$$

Introducing in Eq. (11b) the expressions for N and V_h from Eq. 's (16) and (17) we get the distance to the rotation centre:

$$e = \frac{A_2}{A_1+A_2}d\left(1 - 2\frac{b\xi}{h\theta_h}\right) + \frac{l}{\theta_u}\xi b$$

The deduction given above holds even if θ_u or θ_l are Zero. $\theta_l = 0$ gives e = neg. e. g. the rotation centre will be above the lateral stiffening. As the aerodynamic stability is much increased by the introduction of a lower lateral system, e. g. $\theta_l > 0$, the normal situation will be $\frac{d}{2} \geq e \geq 0$.

Shear resistance θ.

For various lattice systems Fig. 17 the shear resistance is given by the formulas:

Fig. 17 a)
$$\theta = \frac{E}{G}\frac{4\lambda}{b\left(\frac{1}{A_c} + \frac{1}{A_D\sin^3\alpha}\right)} \qquad (22)$$

b) "
$$\theta = \frac{E}{G}\cdot 2A_D\cdot\sin^2\alpha\cos\alpha$$

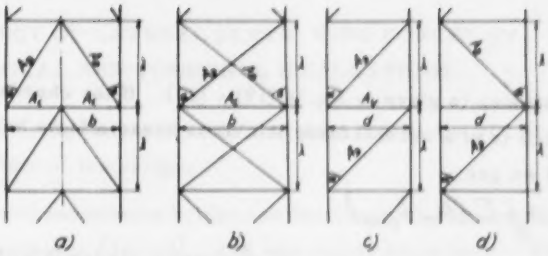

Fig. 17. Common lattice systems.

Fig. 17 c)
$$\theta = \frac{E}{G}\,\frac{\lambda}{d\left(\frac{1}{A_V} + \frac{1}{A_D \sin^3\alpha}\right)} \qquad (22)$$

d)
$$\theta = \frac{E}{G}\, A_D \sin^2\alpha \cos\alpha \qquad "$$

An optimum effect will arise when the angle α is within the limits 40 - 55°.

Effect of webs.

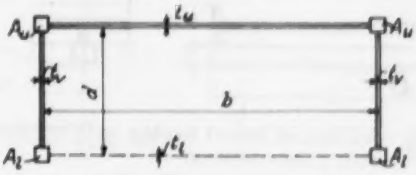

Fig. 18. Cross section of bridge.

With a cross-section as given in Fig. 18 the formulas (19) - (21) are still valid if we introduce:

$$\left.\begin{aligned} A_1 &\approx A_u + \tfrac{1}{6}\, b\, t_u + \tfrac{1}{6}\, d\, t_v \\ A_2 &\approx A_l + \tfrac{1}{6}\, d\, t_v + \tfrac{1}{6}\, b\, t_l \end{aligned}\right\} \qquad (23a)$$

The shear resistance will be given by

$$\theta_v = d\, t_v \;;\; \theta_u = b\, t_u \;;\; \theta_l = b\, t_l \qquad (23b)$$

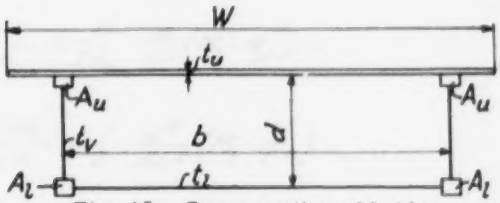

Fig. 19. Cross section of bridge.

A section as given in Fig. 19 will have

$$A_1 \approx A_u + \tfrac{1}{6}\, d\, t_v + \tfrac{1}{6}\, t_u\, w \left(\frac{w}{b}\right)^2 \qquad (24)$$

$$\Theta_u \approx b \cdot t_u \tag{24}$$

Torsional stiffness is given in Eq. 's (19) - (20). If the chords are hollow or the bridge deck is of a considerable thickness these effects have to be considered, and we get

$$I_D = 2db\xi + \frac{1}{G}\Sigma (G_n I_{Dn}) \tag{20a}$$

In small suspension bridges with a single lateral girder it will be of great effect to have cross beams which are of great torsional stiffness, see Fig. 20 The total effect will then be

$$I_D = \frac{1}{G}\left[\Sigma (G_n I_{Dn}) + G_{CB} \cdot I_{DCB} \cdot \frac{b}{\lambda}\right] \tag{20b}$$

where I_{DCB} is the torsional stiffness of a cross beam and λ the distance between the beams.

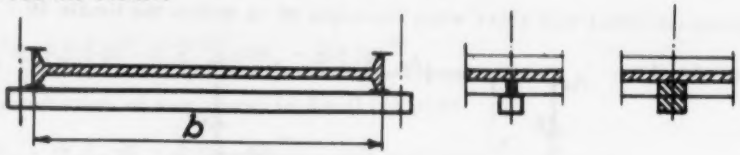

Fig. 20. Section of small bridge with torsional stiff cross beams.

4. EFFECT OF LATERAL STATIC WIND FORCES ON VERTICAL AND TORSIONAL OSCILLATIONS.

In a suspension bridge exposed to lateral wind forces we will have stresses in the lateral system of the bridge.

The calculation of suspension bridges under a lateral static wind force is well known in the literature [10, 14] , and will not be given here. The bending moment in the lateral system is called M_l. The existense of M_l will have an effect on the natural frequencies.

In a bridge oscillating in a pure vertical oscillation M_l will produce a torsional moment on an element dx, see Fig. 21a.

$$dM_T = d(M_l \cdot \eta_v') \tag{1}$$

e. g. when we have static lateral wind moments a pure vertical oscillation can not exist.

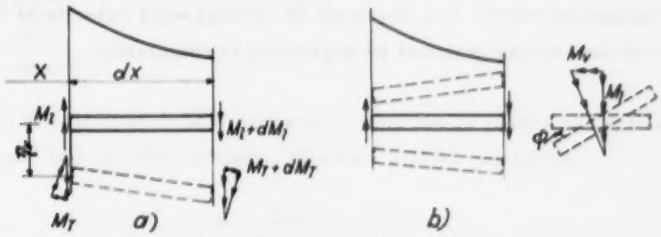

Fig. 21. Effect of moments due to lateral wind.

In a bridge oscillating in a pure torsional oscillation M_l will produce a vertical moment on the element, see Fig. 21b.

$$dM_v = d(M_l \cdot \varphi_T) \tag{2}$$

i. e. a pure torsional oscillation will not exist.

The moments d M_T and d M_v may be replaced by forces or loads in the suspender plan

$$w_{M_l} = \frac{dM_T}{dx \cdot 2b_c} = \frac{1}{2b_c} \frac{d}{dx}(M_l \cdot \eta_v') \tag{3}$$

and

$$w_{M_l} = \frac{1}{2} \frac{d^2(M_v)}{dx^2} = \frac{1}{2} \frac{d^2}{dx^2}(M_l \cdot \varphi_T) \tag{4}$$

where φ_T is the angular amplitude of the torsional oscillation.

Eq. (3) and (4) demonstrate that all oscillations will be coupled. The bridge will have increased hanger forces:

$$W_l = \pm \frac{1}{2b_c} \frac{d}{dx} (M_l \cdot \eta_v') + \frac{1}{2} \frac{d^2}{dx^2} (M_l \cdot \varphi_T) \qquad (5)$$

with + on the lee side and - on the windward side.

All problems connected with the aerodynamic stability pressuppose that there is a lateral wind and consequently that it exists a lateral moment M_l. The exact finding of the coupled frequencies etc. will be most complicated.

However, our knowledge of the aerodynamic stability will be founded on wind tunnel tests. To have correct tests we need models mounted with correct natural frequencies in still air and where the frequencies change with increasing wind forces as may be deduced by the Equations (1) - (5). As will be seen later in chapt. 6. 3. it is comparatively easy to give the model such a mounting.

The W_l forces, Eq. (5), will usually be small compared to the weight of the bridge. The effect of lateral static wind forces will be small for most bridges, and only seldom it results in a decrease of critical wind velocity of 10%, compared to the results obtained by neglecting it completely.

5. EFFECT OF SIMPLIFICATIONS.

5.1. Shear deformation in stiffening truss.

In Equation (1.5) is given the relation between deflection, shear and moment.

Introducing $\eta_t = \eta \sin \omega t = \sum a_n \sin n\pi \frac{x}{l} \cdot \sin \omega t$

gives

$$M_t = M \sin \omega t = \left(JE \frac{\pi^2}{l^2} \sum \frac{n^2}{1 + \frac{JE^2\pi^2}{GF \cdot l^2} \cdot n^2} \cdot a_n \sin n\pi \frac{x}{l}\right) \sin \omega t$$

and

$$M'' = - JE \frac{\pi^4}{l^4} \sum \frac{n^4}{1 + R \cdot n^2} a_n \cdot \sin n\pi \frac{x}{l} \qquad (1)$$

where $R = \frac{\pi^2 JE}{GF \cdot l^2}$

Instead of the coefficient $\alpha = \frac{\pi^4 JE}{m l^4}$ we get the more correct value

$$\alpha \frac{1}{1 + Rn^2} \qquad (2)$$

However, R will always be small and as only lower modes of oscillations are of technical interest the influence of shear will be negligible.

5.2. Cable force.

Introducing $\eta_t = \eta \sin \omega t = \sum a_n \sin n\pi \frac{x}{l} \cdot \sin \omega t$

in Eq. (1. 11a) results in

$$\int_c^{c'} \frac{H_{st} \cdot \sec^3 \varphi}{E_c A_c} dx \approx H_{st} \frac{L_s}{E_c A_c} = \left[\frac{32}{\pi l} \sum \frac{a_n}{4n} \left(1 - (-1)^n\right) \sin \omega t + \frac{\pi^2}{4l} \sum n^2 a_n^2 \cdot \sin^2 \omega t\right] \qquad (3)$$

This equation demonstrates that $\eta_t = \eta \sin \omega t$ is an approximation as H_{st} does not have a variation only with $\sin \omega t$. The last term in Eq. (3) is the effect of the term $\frac{1}{2} \int (\eta')^2 dx$ in Equation (1. 11a), and it is practically equivalent to the introduction of:

$$H_w + \frac{\pi^2 E_c A_c}{8 \cdot l \cdot L_s} \sum n^2 a_n^2 \qquad (4)$$

instead of H_w in our formulas.

The difference will increase with a_n. However, even for a_n values which are impossible in a sound structure the last term in Eq. (4) will be small against H_w and is in consequence neglected.

5.3. Cable slope φ.

In deduction of our equations we introduced the simplification:

$$\frac{d}{dx}(\eta' \sec^2\varphi) \approx \eta'' \sec^2\varphi_m \qquad (5)$$

Instead of solving Eq. (2. 7b) we might as well have solved Eq. (2. 7a). The solution of the more correct Equation (2. 7a) may be obtained in the same manner as for static loads [10]. The results will differ less than 2 - 3% from those given in Chapt. 2.

As this error is of the same magnitude or less than other neglected effects (elongation and spacing of hangers, uncertanties in J and $A_c E_c$, etc.) it seems to be little reason for the use of an extremely laborious "exact" solution.

5.4. Lateral movements.

In Chapt. 3 we neglected that the torsion might give a movement and sidesway to the suspended system. and in turn produce a sidewise inclination of the hangers.

However, for bridges with an ⌐¯¯¯¯¯¯¬ section and only one lateral stiffening girder the centre of rotation may be situated so high that the lateral movement might give a small effect. Being of no technical importance it will be neglected here.

Pure lateral oscillations of a suspension bridge will not be an actual mode of oscillation. However, the calculation of the natural frequencies for such an oscillation is comparatively easy [15], but shall not be given here.

6. MODEL TESTS FOR SUSPENSION BRIDGES.

6.1. Models and model dimensions.

The most convenient testing will be with models working in air with normal pressure and temperature. For such a model we have the following connection between bridge and model dimensions

Length, width, etc.	$b_m = \frac{1}{n} b$	(1)
Time	$t_m = \frac{1}{k} t$	
Circular frequency	$\omega_m = k\omega$	
Velocity	$V_m = \frac{k}{n} V$	
Acceleration	$a_m = \frac{k^2}{n} a$	
Weight per unit length	$w_m = \frac{1}{n^2} w$	
Mass per unit length	$m_m = \frac{1}{n^2} m$	
Mass of gyration per unit length	$\mathcal{M}_m = \frac{1}{n^4} \mathcal{M}$	

The index m is used for model, n being the reduction factor in length, and k the reduction factor in time.

Between the wind velocity v, width b and frequency N we have

$$\frac{V_m}{N_m b_m} = \frac{V}{N b} \tag{2}$$

presupposing that the wind flow will be turbulent and independent of Reynolds number. This assumption will for the most suspension bridges be well established.

The energy given to a unit length of bridge or model per vertical oscillation will be

$$E_v = F(\eta, b) v^2$$

$$E_{vm} = F(\eta_m, b_m) V_m^2 = \frac{k^2}{n^4} E_v \tag{3a}$$

The damping effect etc. consume the energy

$$E_\delta = m \cdot \omega^2 \eta^2 \cdot \delta$$

$$E_{\delta m} = m_m \omega_m^2 \eta_m^2 \cdot \delta_m = \frac{k^2}{n^4} \cdot m \cdot \omega^2 \eta \cdot \delta_m \tag{3b}$$

The relation between introduced energy and consumed energy have to be the same for bridge and model; e. g.

$$\frac{E_v}{E_{vm}} = \frac{E_\delta}{E_{\delta m}} \quad \text{or} \quad \delta_m = \delta \tag{4}$$

It will be an approximation on the safe side if we introduce $\delta_m \leq \delta$ as a rule: The total damping of the model shall be less or like the damping of the bridge.

For a torsional oscillation we have in the same manner

$$E_T = F_T(\varphi b^2)v^2;\ E_{Tm} = F_T(\varphi \cdot b_m^2)v_m^2 = \frac{k^2}{n^4}E_T$$

$$E_{T\delta} = \omega_T^2 \mathcal{M} \cdot \varphi^2 \delta_T;\ E_{T\delta m} = \omega_{Tm}^2 \cdot \mathcal{M}_m \cdot \varphi^2 \delta_{Tm} = \frac{k^2}{n^4}\omega_T^2 M \varphi^2 \delta_{Tm} \tag{5}$$

Demanding the same relation between introduced and consumed energy we get

$$\delta_{Tm} = \delta_T \tag{6}$$

or with an approximation to the safe side

$$\delta_{Tm} \leq \delta_T$$

The structural damping of the model should be equal to or less than the structural damping of the bridge.

The bridge damping depends on the bridge construction and is relatively little known. However, some values measured on bridges will be found in the literature [2, 5, 13].

For the decrement δ we may use as lower limit:

Vertical oscillations with one node	$\delta = 0,07$
Vertical oscillations with 2 or more nodes	$\delta = 0,04$
Torsional oscillations	$\delta = 0,05$

It is relatively simple to get these or smaller values for the decrement in a model.

6.2. Full model and sectional model.

In tests using a full model of the bridge there will be an automatic inclusion of all secondary effects as the effect of lateral wind (Chapter 4) and the effect of all simplifications (Chapter 5). The first effect being dominant. However,

if the model shall not be too small a full model will be an expensive model, and especially any changes will be a slow process taking much time. However, there has been built some full models [2, 6, 7, 16] . Comparisons of results obtained with full models and sectional models demonstrate a very good correlation and further that the sectional models give sufficiently accurate information.

With models is henceforth always thought of sectional models.

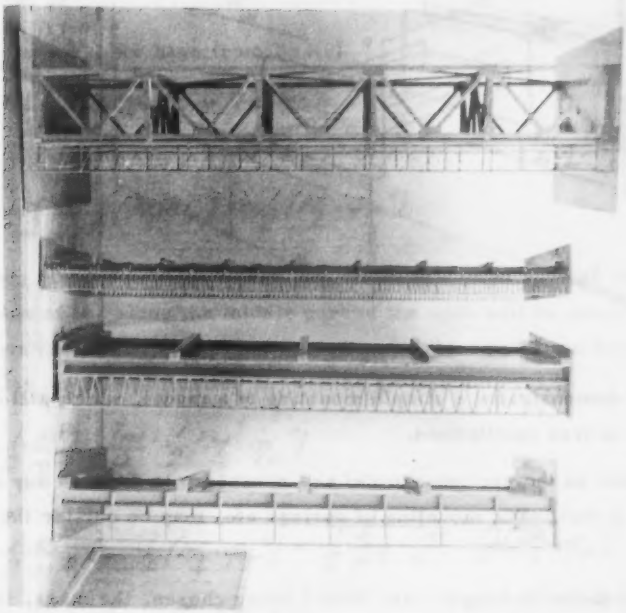

Fig. 22. Models of some of the investigated bridges.

Sectional models representing only a short length of the bridge, see Fig. 22, give rise to the following errors:

a) Neglection of effect of lateral wind (Chapt. 4)

b) Neglection of secondary effects (Chapt. 5)

c) Neglection of the different shape of a vertical and torsional oscillation.

The errors may be improved by the following measurement:

a) Improved mounting of the model as demonstrated in Chapt. 6. 3. For most bridges a sufficient accuracy is obtained without this refinement.

b) Inclusion of the secondary effects in the calculation of natural frequencies.

c) This approximation is on the safe side [3, 4, 16, 17]. However, the effect will usually be small.

6.3. Mounting of model.

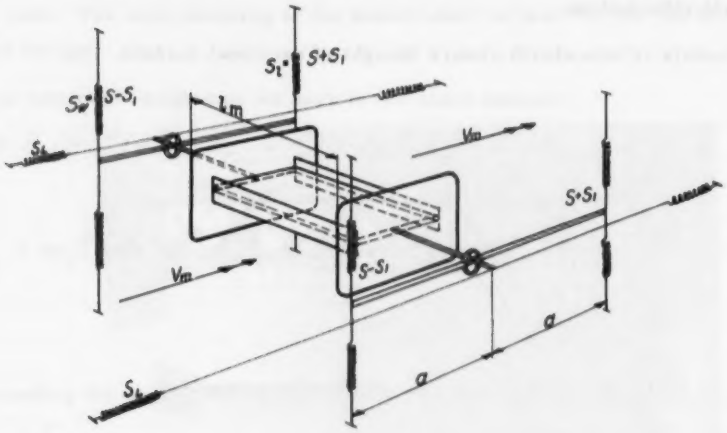

Fig. 23. Mounting of sectional model.

In Fig. 23 is demonstrated a simple mounting of a model, which will have 2 or 3 degrees of free oscillations.

The end shields on the sectional model are necessary to depress any end effect on the model. The mounting of springs, etc., may be outside the wind stream.

The reduction factor in length n and time k being chosen, the mass, frequency, etc., of the model are given from Eq. 's(1).

The lateral springs may usually be neglected e. g. we introduce $S_l = \infty$, and get a system with two degrees of freedom, vertical and torsional oscillations. Lateral oscillations are never observed on an actual bridge, however, as the calculation of lateral oscillations are comparatively easy [15] it might very well be included in the tests.

The spring constant S, is calculated from the vertical frequency, and the spring distance 2a from the torsional frequency. The axis going through the centre of rotation for pure torsional oscillations.

The spring constant S_l is determined from the effect of lateral static wind, Chapt. 4, Eq. (4. 3) - (4. 5).

With a known wind velocity on the bridge W_l may be calculated from Eq. (4. 5) for a given vertical or torsional oscillation.

$$W_{lv} = \pm \frac{1}{2 b_c}\left(\frac{d}{dx}(M_l \eta_v')\right) \; ; \; W_{lT} = \frac{1}{2}\frac{d^2}{dx^2}(M_l \varphi_T) \qquad (6)$$

With springs mounted at distances 2a, and reduction factor in length n and time k given, we have for the model

$$S_{lv} = \frac{1}{2}\frac{k^2}{n^2} W_{lv} \cdot l_m \frac{b_{cm}}{a} \quad \text{resp.} \quad S_{lT} = \frac{1}{2}\frac{k^2}{n^2} W_{lT} \cdot l_m \qquad (7)$$

In W_{lv} and W_{lT} we have from Eq. (6)

$$W_{lv} = \pm \frac{1}{2 b_c} \cdot \frac{d}{dx}(M_l \cdot \eta_v') \approx \pm \frac{1}{2 b_c}(M_l \cdot \eta_v'')$$

$$W_{lT} = + \frac{1}{2}\frac{d^2}{dx^2}(M_l \varphi_T) \approx \frac{1}{2}(M_l \cdot \varphi_T'')$$

For long slender bridges where this effect will be of special interest, the variation of M_l along the middle part of the span will be small [10, 14], and the term containing the second derivative of the oscillation becomes dominant. With this last simplification S_l will be given by:

$$\left.\begin{aligned} S_l &\approx \frac{1}{2}\frac{k^2}{n^3} \cdot \frac{l_m}{a} \cdot \frac{1}{2}(M_l \cdot \eta_v'') \\ S_l &\approx \frac{1}{2}\frac{k^2}{n^2} l_m \frac{1}{2}(M_l \cdot \varphi_T'') = \frac{1}{2}\frac{k^2}{n^3}\frac{l_m}{a} \cdot \frac{1}{2}(M_l \cdot \eta_v'') \end{aligned}\right\} \qquad (8)$$

with oscillations n. a. $\varphi_T = \eta_v = 1$.

A sufficiently accurate mounting is possible with an arrangement as shown in Fig. 23. Still a better result, using the correct effect of M_l, will be possible with use of more springs. However, there seems to be little reason for this improvement.

As the wind moment M_l approximately varies with the square of the wind velocity, the springs should be adjusted with changes in velocity. However, as the effect of S_l proves to be small, a more rapid investigation is to make separate tests with S_l equal to Zero and S_l equal to its maximum possible value. We then have the necessary limits to see the effects of the lateral wind pressure.

The tests with various suspension bridges carried out for the Norwegian

Administration of Public Roads gave as a result that the critical wind velocities are somewhat decreased by this effect. However, the decreased velocity will only seldom be below 90% of the results obtained by neglecting the effect of the lateral moment M_l. For preliminary investigations, see Chapt. 7, this simplification always seems to be justified.

In Fig.'s 27-29 are represented the results of som tests carried out with springs $S_w = S_l$ and $S_w = \frac{1}{2}S_l$. As demonstrated by the tests the decrease in velocity are small and of minor importance for the lower values of critical velocity.

It will only seldom occure that the lateral wind will have an effect which compares to tests with $S_w \approx \frac{1}{2}S_l$, however, an interpolation between the results obtained with $S_w = S_l$ and $S_w = \frac{1}{2}S_l$ should be sufficiently accurate for our purpose.

7. TEST RESULTS.

7.1. Systematic tests with simplified models.

During the years 1954-58 the author, on behalf of the Norwegian Administration of Public Roads, carried out a number of wind tunnel tests for new and older suspension bridges. Some of the models used are shown in Fig. 22.

The tests demonstrated clearly that the effect of open trusses, handrails, etc., are small. In consequence systematic tests with simplified bridge sections were made, see Fig. 24. The purpose being to get information for predicting the critical velocity for bridges to be built in the future.

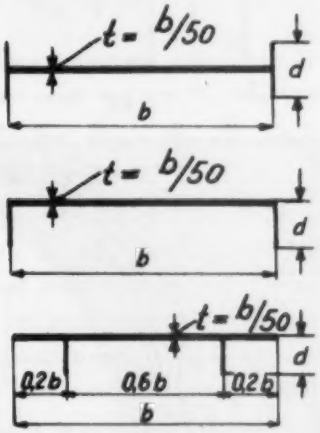

Fig. 24. Cross sections used in systematic tests.

Comparisons between tests on complete models and simplified models, where handrails, trusses, etc., are neglected, proved that the error by using the latter are within ± 10%, this value being reached only for bridges with relatively compact handrails and trusses.

Representation of the results in dimensionless diagrams have been possible by using the critical velocity predicted by the "Flutter" theory V_F as a reference value, when investigating a coupled or torsional oscillation, see Eq. (1), (2), and (3). When investigating vertical oscillations a similar reference value is used, see Eq. (4), (5).

7.2. Coupled oscillations. Flutter velocity V_F.

The late Dr. Friedrich Bleich introduced the Flutter-theory in the investigation of critical wind velocity for suspension bridges [3, 4, 16, 17]. The

$S = 0,001283 \frac{273}{273 + t} \cdot \frac{B}{B_o}$ t/m³

S = Specific weight of air

w = Weight of bridge - pr. m. and pr. cable

r = Mass radius of gyration

$\omega_v = \frac{2\pi}{T_v}$ Circular frequency in vertical oscillation

$\omega_T = \frac{2\pi}{T_T}$ " " in torsional oscillation

$\omega_F = \frac{2\pi}{T_F}$ " " in Flutter oscillation

b = Width of bridge deck

FLUTTER VELOCITY V_F.

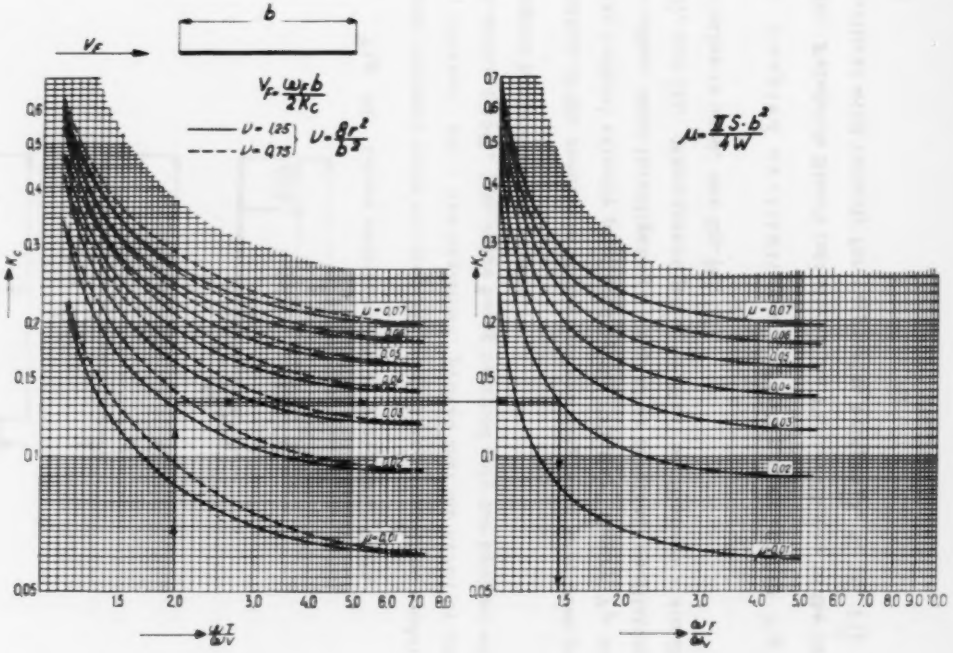

Fig. 25

Flutter-theory, well known from aerodynamics [18, 19], gives the critical wind for a section consisting of a thin plane slab, and with the wind direction coinciding with the plane of the slab. This Flutter velocity V_F is readily calculated as demonstrated by Bleich [3, 4]. However, the calculation is greatly simplified by representing the results in a diagram as shown in Fig. 25. An interpolation in the Tables given by Bleich [3, 4] will usually be too inaccurate, and a direct calculation will be very tedious without giving any increase in accuracy compared with the diagram.

An approximate value of V_F is given by the following empirical formulae:

$$V_F = 0,44\ \omega_T\ b\ \sqrt{\left(1-\left(\frac{\omega_v}{\omega_T}\right)^2\right)\ \frac{\sqrt{\nu}}{\mu}} \qquad (1)$$

The error in this formulae decreases with $\frac{\omega_v}{\omega_T}$. The error will for values $\omega_v/\omega_T \approx 0,7$ be ~ 4 per cent, and for $\omega_v/\omega_T \approx 0,5$ be $\sim 1,5$ per cent.

The use of Flutter velocity V_F as a reference value for the critical velocity

$$V_c = k\ V_F \qquad (2)$$

works very well for the various values of d/b, see Fig. 24 and Fig.'s 26-29. For higher values of d/b, f. inst. d/b≈0,1, it might as well have been used for reference the critical velocity of pure torsional oscillations. With increasing values of d/b the oscillations will change from typical coupled oscillations, as the flutter oscillations, to more and more dominating torsional oscillations. However, the tests demonstrate that higher values of d/b should be avoided. Of interest is to note that increasing the d/b from 0,05 to 0,1 usually will decrease the critical velocity, and an increase of d/b from 0,1 to 0,2 usually will give a slight rise of critical velocity as the flutter velocity V_F will be rised with increasing stiffness of the bridge and the multiplier k, Eq. (2), will vary as seen in Fig.'s 30-38.

With pure torsional oscillations the formula (1) is reduced to

$$V_T = 0,44\ \omega_T\ \ b\ \sqrt{\frac{\sqrt{\nu}}{\mu}} \qquad (3)$$

and the critical velocity will be

$$V_c = k_T\ V_T \qquad (4)$$

However, when a pure torsional oscillation gives the lower value of V_c the wind tunnel tests will give this V_c automatically. As the difference in Eq. (1) and (3) is insignificant in most cases all following definitions and tests will be common for coupled and pure torsional oscillations.

7.3. Coupled oscillations. Critical velocity.

It is necessary to define what is meant by critical velocity for a bridge. There are three possible views:

1. An oscillation which is seen and felt by the trafficants, but not being dangerous for the bridge.
2. An oscillation which a well constructed bridge should stand for several hours without severe damages.
3. An oscillation which in a short time should destroy the bridge.

The start and building up of oscillations may also be an important point. There is always a possibility that a gust of short time duration will start an oscillation, and the further development depends then on the mean value of the wind velocity in the following 5 - 10 - 15 minutes, see Chapt. 8.

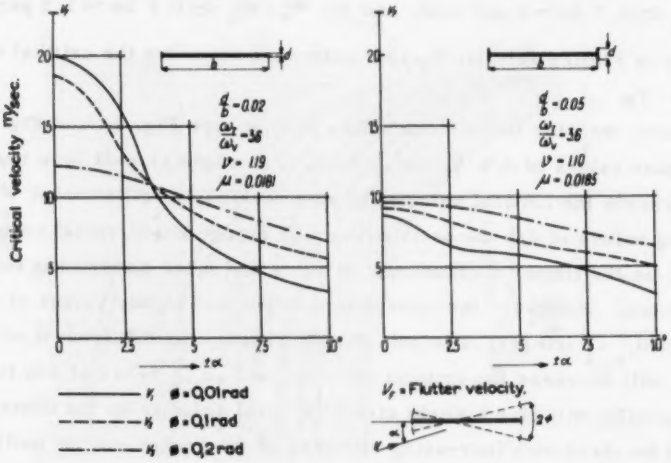

Fig. 26. Examples of test results.

With a background as described above the following definitions of critical velocity are made for coupled torsional - vertical oscillations or torsional oscillations:

V_1 is the highest wind velocity where an initiated oscillation of $\pm$ 0,01 rad (0, °35) will be stable or decrease.

V_2 is the wind velocity where an initiated oscillation of $\pm$ 0,1 rad (5, °44) will be stable or decrease.

V_3 is the velocity where an initiated oscillation of $\pm$ 0,2 rad (11, °27) will be stable or decrease.

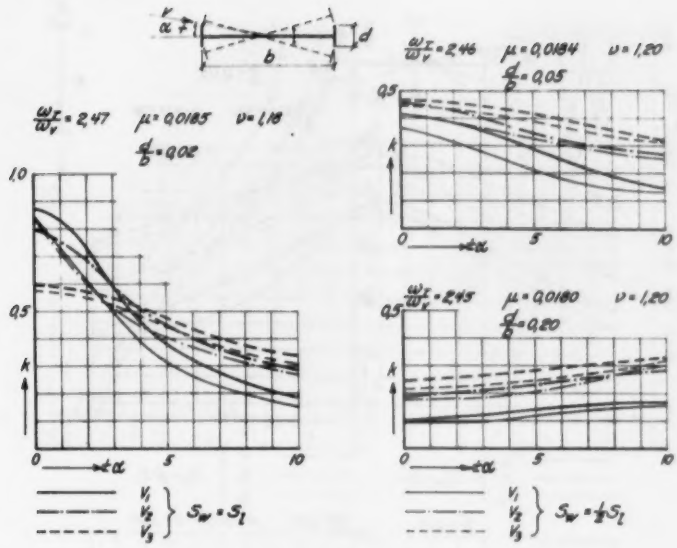

Fig. 27. Test results with two different mountings of model.

In Fig.'s 26-27 are given the variation of V_1 ; V_2 ; V_3 with the angle of attack and the factor d/b for some symmetrical ⊢——⊣ sections. In Fig. 28 and 29 are given the same for some of the ⌐——¬ and ⊤——⊤ sections.

If we demand that the oscillations should be built up by the steady wind we would get somewhat higher V_1 - V_3 values. However, remembering the nature of the wind, the given definition was found to be better.

V_1 - V_3 are defined only by the rotation. The oscillations will be coupled or nearby torsional oscillations, and a definition by the angular rotation will give the most characteristic description of the oscillation.

The results of the testing program are given in the diagrams Fig.'s 30-38.

In Fig.'s 27-29 are demonstrated the effect of lateral wind, see Chapt. 4 and Chapt. 6, 3. In most cases this effect of lateral wind gives a slight decrease in critical velocities, usually of magnitude 5 to 10 per cent, see Chapt. 6, 3.

The main part of the tests were made with models having a mass ratio μ, see diagram Fig. 25, about 0,018. This value was chosen while a greater part of the Norwegian suspension bridges have this mass ratio.

The distribution of the mass is given by the ratio ν, see diagram Fig. 25. In the same manner this ratio was about 1,1 for the greater part of the tests.

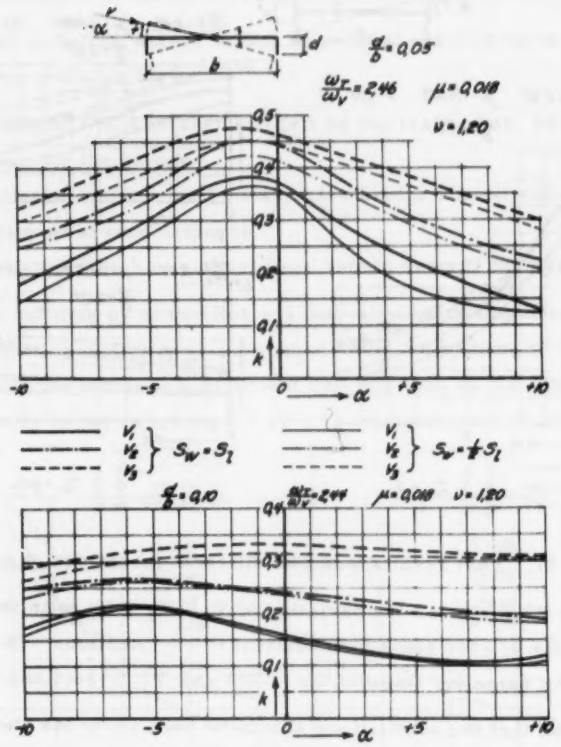

Fig. 28. Test results with different mounting of model.

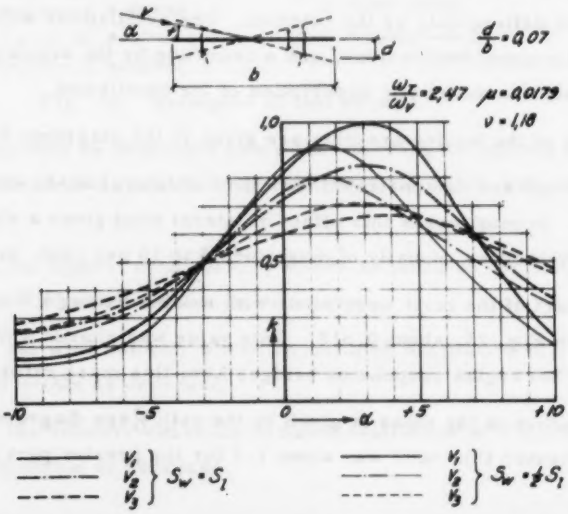

Fig. 29. Test results with different mounting of model.

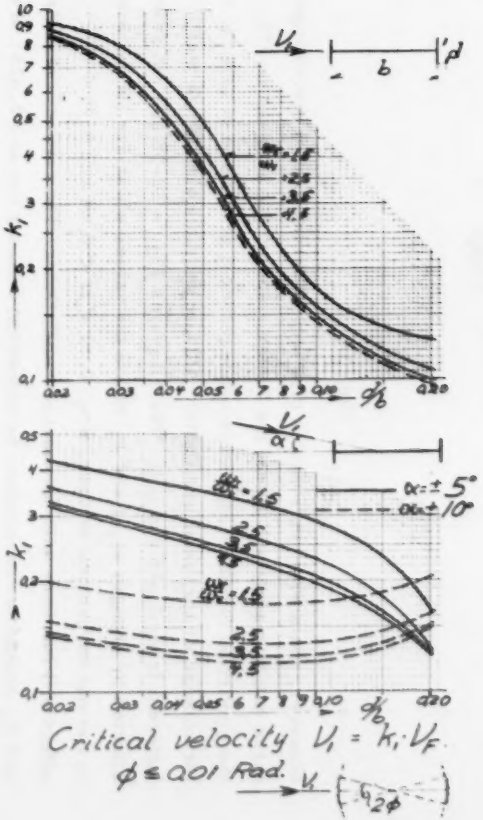
Critical velocity $V_1 = k_1 \cdot V_F$
$\phi \leq 0.01$ Rad.

Fig. 30

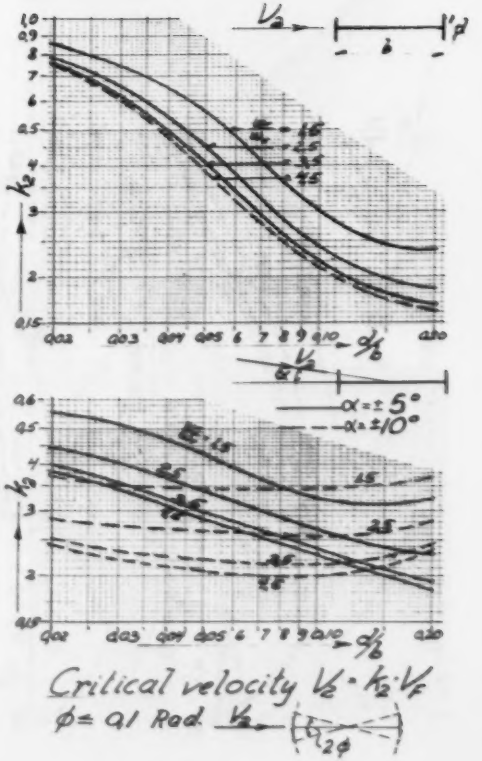
α = ± 5°
α = ± 10°
Critical velocity $V_2 = k_2 \cdot V_F$
$\phi = 0.1$ Rad.

Fig. 31

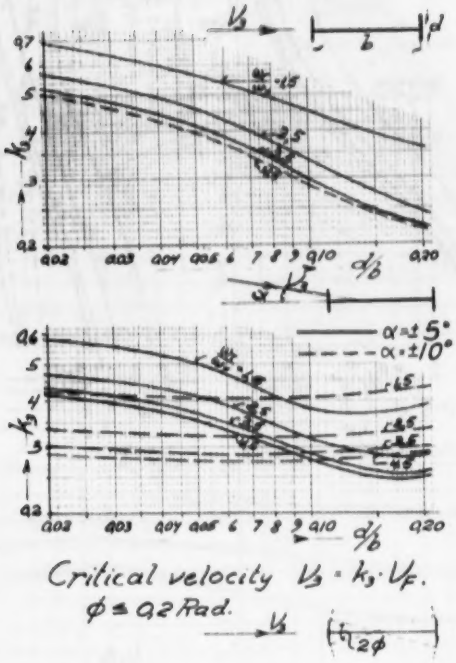

Fig. 32.

However, tests with other values of μ and ν demonstrated that changes in these ratios mainly will affect the flutter velocity V_F as given in Fig. 25 or in the empirical formula (1), and in consequence a prediction of critical velocities for coupled or torsional oscillations will be possible also for μ and ν values different from 0,018 and 1,1. The diagrams Fig.'s 30-38 are not markedly affected by changes in μ and ν_1 within the values which are likely to occure in normal suspension bridges, e.g. $0,01 < \mu < 0,04$ and $0,75 < \nu < 1,5$. The effect will increase with increasing oscillations. The critical velocities V_2 and V_3 should in consequence be somewhat reduced for $\mu > 0,025$; $\nu < 1,0$. The reduction will seldom gain a value of 10%.

A representation of more complete diagrams giving factors K as functions of the independent variable μ and ν will be beyond the need of the bridge builder, and remembering the difference in natural wind and the test wind, without sense.

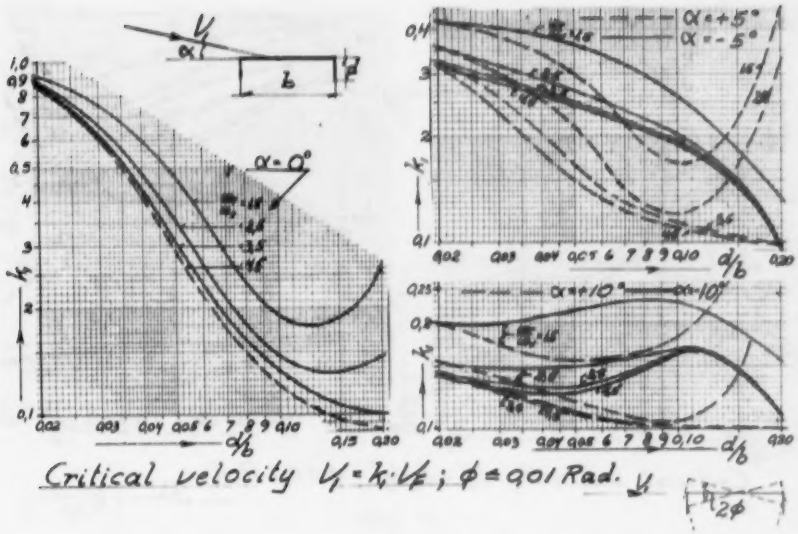

Fig. 33

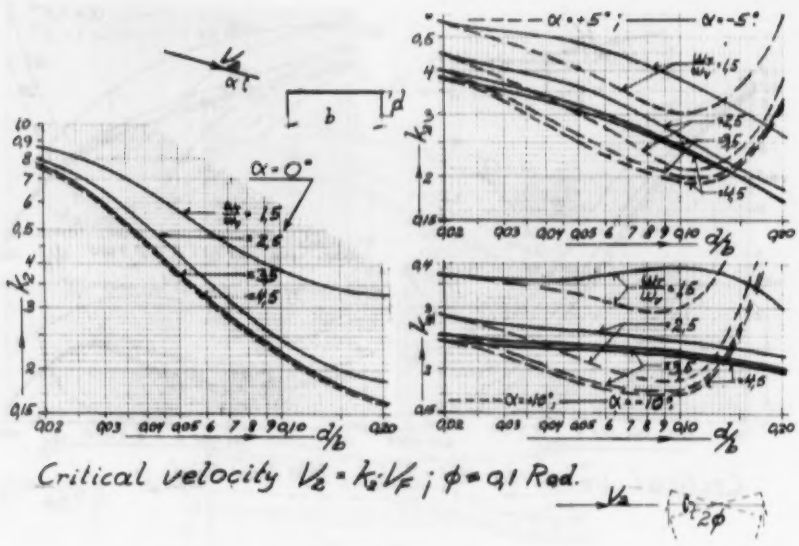
α = 0°
α = +5°
α = -5°
α = +10°
α = -10°
b
d
d/b
Critical velocity $V_2 = k_3 \cdot V_F$; $\phi = 0{,}1$ Rad.

Fig. 34

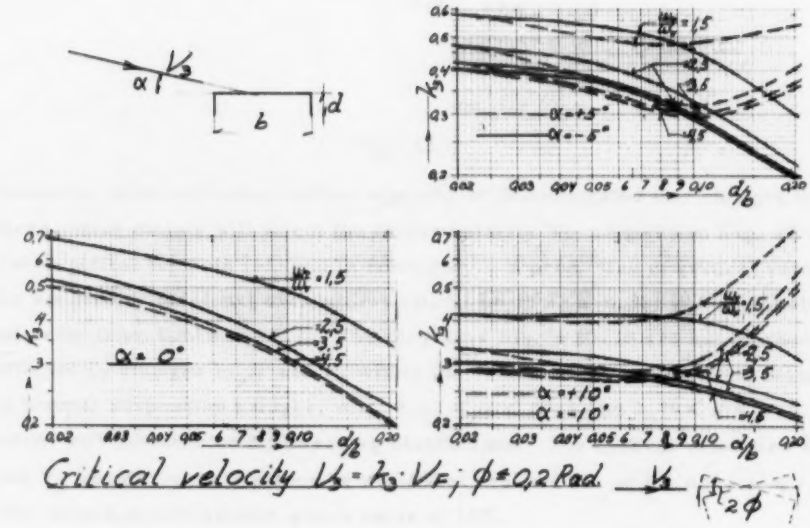
α = 0°
α = +5°
α = -5°
α = +10°
α = -10°
b
d
d/b
Critical velocity $V_3 = k_3 \cdot V_F$; $\phi = 0{,}2$ Rad.

Fig. 35

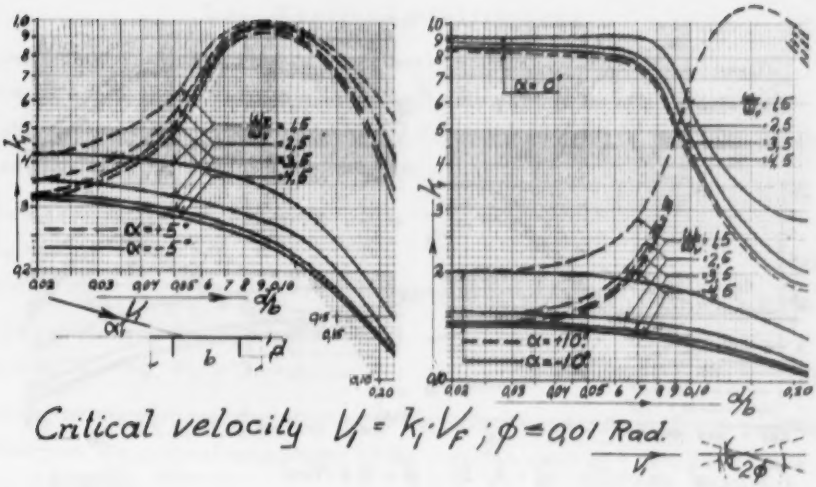

Critical velocity $V_1 = k_1 \cdot V_F$; $\phi = 0{,}01$ Rad.

Fig. 36

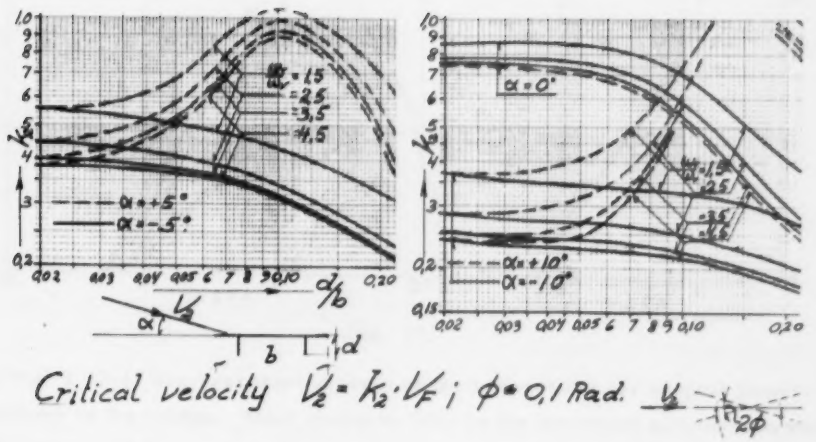

Critical velocity $V_2 = k_2 \cdot V_F$; $\phi = 0{,}1$ Rad.

Fig. 37

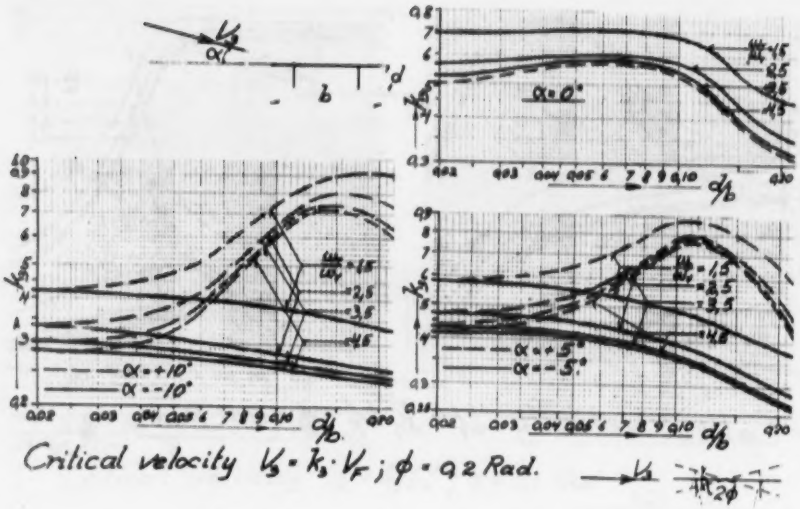

Fig. 38

7.4. Vertical oscillations.

Compared with the coupled and torsional oscillations the vertical oscillations are of minor interest. They will only seldom be of a catastrophic nature. However, they are frequently observed on bridges, but have never been the main reason for a disaster.

Similar to Eq. (1) we may write

$$V_v = \ldots\ldots\ldots\ldots \omega_v \; b \qquad (5)$$

and we shall use this value as a reference value.

The critical velocity will be

$$V_c = k_v \, V_v = k_v \, \omega_v \, b \qquad (6)$$

To define the critical wind similar to the definitions in Chapt. 7.3 is possible. However, the critical amplitudes of the structure will be a function mainly of the span length.

The tests are therefore not run with given defined amplitudes, but the amplitudes are represented as a function of the shape and the width of the bridge deck. See Fig.'s 39-44.

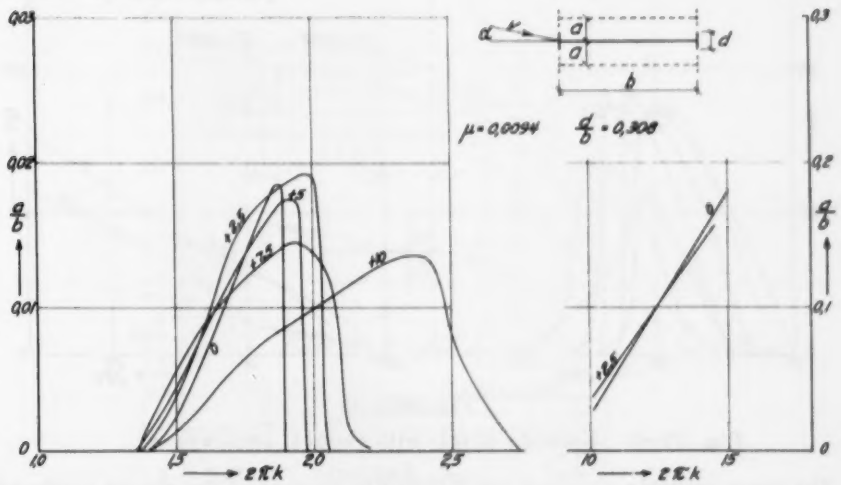

Fig. 39.

In Fig.'s 39-41 are represented some of the test results for various cross-sections of the bridge. Most characteristic is the existense of intervals where the bridge will be stable and no oscillation can excist for a steady wind. However, with increasing wind velocities the intervals where the bridge is unstable give increasing amplitudes.

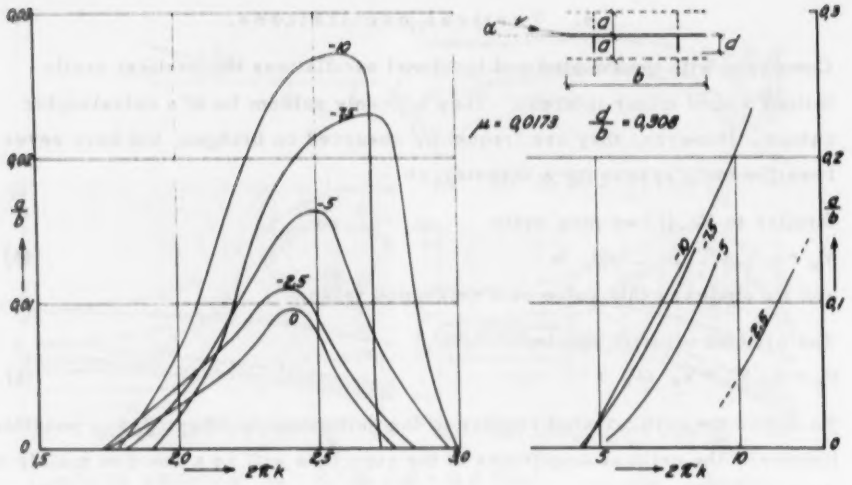

Fig. 40.

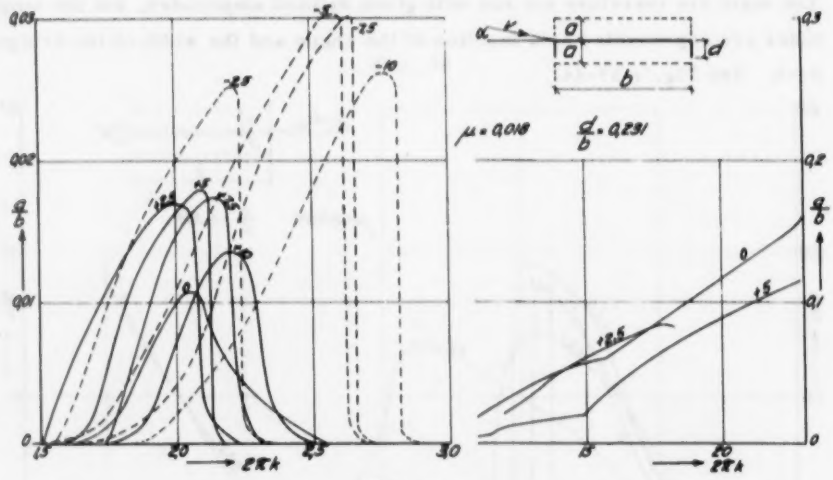

Fig. 41.

Fig. 39-41: Example of test with vertical oscillations.

The lower unstable intervals are difficult to observe as the energy produced by the wind is insufficient to give rise to oscillations which can clearly be observed.

As may readily be seen from the diagrams Fig.'s 42-44, all the tested cross-sections have an unstable area for $0,25 < k_v < 0,45$, the oscillations, however, are small with amplitudes less than 0,01 b for normal bridges. This oscillations are frequently observed on suspension bridges and may in some

cases prove to be unpleasant for the traficants. However, such small oscillations are never dangerous to the structure and cannot be the cause for any disaster.

Fig. 's 42-44 demonstrate, however, that a further increase of wind velocity may produce dangerous oscillations with increasing amplitudes. This will occure for suspension bridges, where d/b usually is small, when wind velocity corresponds to $k_v = 3,0 - 4,0$.

Compared with the wind velocity which produce coupled- or torsional oscillations we find, however, that the dangerous type of vertical oscillations usually demand a higher wind velocity, and in consequence is of minor interest.

The smaller vertical oscillations produced at wind velocities corresponding to $0,25 < k_v < 0,45$ may, combined with wind gusts, give start to the torsional or coupled oscillations and represent a danger, especially when flutter oscillations and pure vertical oscillations can excist at nearby the same wind.

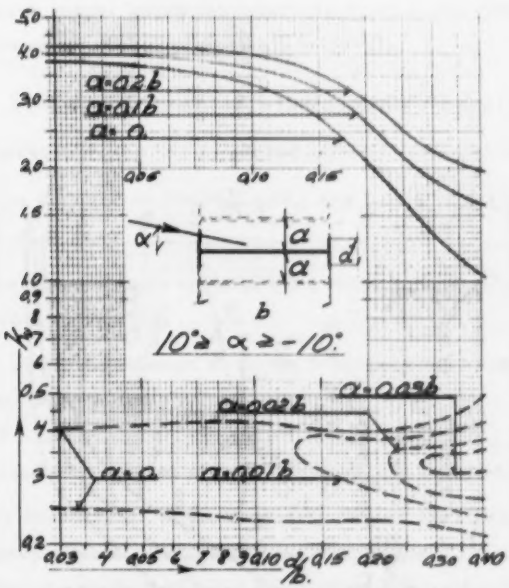

Fig. 42.

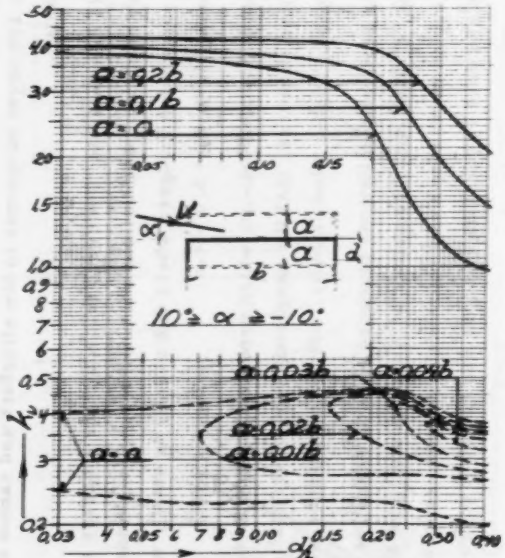
a=0,2b
a=0,1b
a=0
10° ≥ α ≥ -10°
a=0,02b
a=0,01b
a=0
Critical velocity V = k_v · b · w_v .
Oscillation amplitude: a

Fig. 43

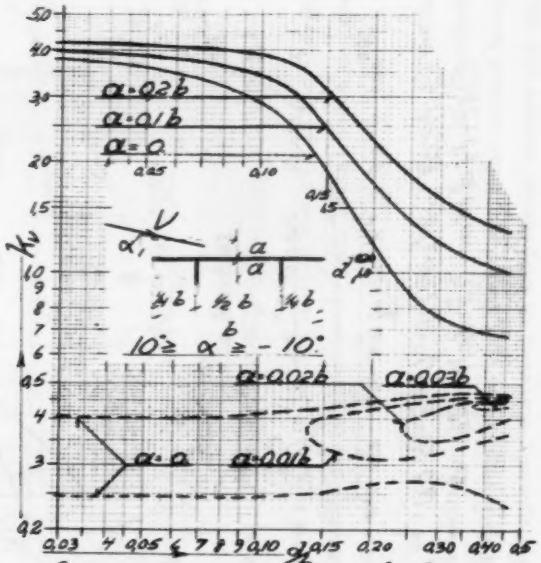
a=0,2b
a=0,1b
a=0
10° ≥ α ≥ - 10°
a=0,02b
a=0,03b
a=0
a=0,01b
Critical velocity V = k_v · b · w_v .
Oscillation amplityde: a.

Fig. 44

Some of the vertical oscillations in the area $0,25 < k_v < 0,45$ excist only when the model is started with a correct amplitude, the diagram will thus perhaps overestimate the chance of this type of oscillations.

The vertical oscillations are dependent on the mass of the bridge e.q. the factor μ, see Eq. (5).

The greater part of the test was made with $\mu = 0,018$, see Chapt. 7.3, and the diagrams Fig.'s 42-44 give the results with this value.

Tests with other mass ratios, e.q. other μ values, demonstrated that the limits between stable conditions and small vibrations are not seriously affected by changes in μ, and that the diagrams in Fig.'s 42-44 may be used for predicting of velocities. However, the amplitude a will be affected, and an approximate value may be given by

$$a_\mu = a_{diagr.} \sqrt{\frac{\mu}{0,018}} \qquad (7)$$

The formula gives reasonable values for $0,01 < \mu < 0,04$.

Bridges having μ values $> 0,03$ may have small none catastrophic vibrations for k values below the intervals given in the diagrams. Compare what is said about the lower unstable intervals.

7.5. Effect of structural damping.

The structural damping has a marked effect on frequencies and oscillations.

All formulae deduced in Chapt. 2 and 3 are based on a structural damping or decrement $\delta \equiv$ Zero.

The real bridge will have a damping as mentioned in Chapt. 6.1 and discussed in the literatur [2, 5, 13].

The effect of the decrement δ on the frequency may approximately be expressed by the formula

$$\omega_\delta \approx \omega \sqrt{1 - \delta} \qquad (8)$$

and corrected frequencies may be found by this formula.

In all tests represented in the diagrams Fig.'s 30-38 and 42-44 the model has been mounted in steel springs and the decrement δ has been about $\delta = 0,04$-$0,05$. When the model has been oscillating with catastrophic movements the decrement has usually been somewhat increased due to secondary effects and vibrations in the mounting of the model.

For most suspension bridges it seems to be safe to use the results obtained

with models having decrement values δ = 0, o4 - 0, o5. However, when we have a bridge where the decrement will be f. inst. δ = 0, 1o - 0, 15 the bridge will stand a much higher critical wind.

The relations between amplitude, critical wind, and decrement are very complicated. A true picture may only be obtained by a close investigation on the actual bridge or on a model. Generally we will have that increasing decrement increases the velocity which is necessary to develop a given oscillation.

Approximately we may introduce

$$V_{\delta cr} = V_{cr} \frac{1}{(1 - \delta)^2} \qquad (9)$$

This formula gives reasonable values for V_2 and V_3 for vertical or coupled oscillations. However, V_1 which defines the limit between stable conditions and very small oscillations is connected with δ in a more complicated manner. The value being generally increased, but a simple and safe rule will be to calculate with V_1 values independent of the δ value.

The formulae (8) and (9) may be used for decrements $0 < \delta < 0, 2$.

7. 6. Concluding remarks.

The use of sectional models introduces some important simplifications.

Such a model will only be correct for bridges where the oscillation modes are identical for vertical and torsional oscillations. This will not take place in actual bridges. In his papers [3, 4], Bleich investigated the effect of these simplifications and his results demonstrate that even a substantial difference in mode of oscillation has only minor effect on the calculated flutter velocity V_F. The sectional model gives the lesser value. The difference may for actual bridges be about 5 - 10 per cent, depending on the stiffness and mass distribution in the bridge, and to the safe side.

As mentioned in Chapt. 6. 2 - 3, the use of sectional models further have the effect that lateral wind forces are neglected. This effect may be corrected by a special mounting of the model, Chapt. 6. 3. However, the diagrams given in Fig. 's 30-38 and 41-42 do not include this effect. The use of diagrams in consequence introduces a simplification. The effect of the lateral wind gives always a reduction of critical wind velocities. The tests made to investigate this effect conclude with a decrease of critical velocities of magnitude 5 - 10 per cent for most bridges. Compare Fig. 's 27-29 where some test results are given. The effect is varying with amplitude and angle of wind attack. Of special importance is that the lateral wind forces always tend to change any

pure vertical oscillation into a coupled or torsional one, thus increasing the chance to get such oscillations in the system.

For most bridges the two simplifications discussed above will counteract each other, and the usual procedure, to neglect both of them, seems to be justified.

7.7. Numerical example.

The use of diagrams will be briefly demonstrated by an example, Brevik bridge. The bridge has a stiffening truss with double lateral system, 3 spans, $l_1 = 85$ m, $l_2 = 272$ m, etc.

Vertical oscillations, Eq. (2.14) and (2.26) give

$$\alpha_1 = \frac{\pi^4 EI_1}{l_1^4 m_1} = 10,22 ; \quad \alpha_2 = \frac{\pi^4 EI_2}{l_2^4 m_2} = 0,064$$

$$\beta_1 = \frac{\pi^2 \bar{H}}{l_1^2 m_1} = 4,73 ; \quad \beta_2 = \quad = 0,461$$

$$\lambda_1 = \frac{8^3 f_1^2}{\pi^2 l_1^3} \cdot \frac{E_i A_c}{L_s m} = 1,47 ; \quad \lambda_2 = 4,70$$

Symmetric oscillation, tower effect neglected, Eq. (2.27)

$$\frac{2 \cdot 1,47}{(\omega^2 - 10,22 - 4,73)} + \frac{4,70}{(\omega^2 - 0,064 - 0,461)} + \frac{4,70}{9(\omega^2 - 81 \cdot 0,064 - 9 \cdot 0,461)} + \\ + \ldots\ldots\ldots\ldots = 1$$

$\omega = 1,99$; $\omega = 3,12$ ..

$\underline{\omega_v = 1,99}$

Torsional oscillations. Eq. (3.8) gives

$$\alpha_{T1} = \frac{\pi^4 EC_{w1}}{l_1^4 \mathcal{M}_1} = 15,5 ; \quad \alpha_{T2} = \quad = 0,10^3$$

$$\beta_{T1} = \frac{\pi^4 (\bar{H} \frac{b_c^2}{2} + I_{D1} G)}{l_1^2 \mathcal{M}_1} = 128 ; \quad \beta_{T2} = \quad = 12,5$$

$$\lambda_{T1} = \lambda_1 \frac{m}{\mathcal{M}} \frac{b_c^2}{2} = 4,00 ; \quad \lambda_{T2} = \quad = 12,8.$$

Symmetric oscillation, tower effect neglected. Eq. (2.27)

$$\frac{2\cdot 4,00}{(\omega^2 - 15,5 - 128)} + \frac{12,8}{(\omega^2 - 0,1o3 - 12,5)} + \frac{12,8}{9(\omega^2 - 81\cdot 0,1o3 - 9\cdot 12,5)} + \ldots\ldots\ldots\ldots = 1$$

$\omega = 4,96$; $\omega = 11,o \ldots$.

$\underline{\omega_T = 4,96}$

Flutter velocity. Fig. 25 or Eq. (7.1)

$\nu = 0,95$; $\mu = 0,o239$; $\frac{\omega_T}{\omega_v} = 2,49.$

From Fig. 25

$K_c = 0,3$; $\frac{\omega_F}{\omega_v} = 1,65$

$\omega_F = 1,65 \cdot \omega_v = 3,28$

$V_F = \frac{\omega_F \ b}{2 \ K_c} = \frac{3,28\cdot 10,3}{2\cdot 0,13} = 130$ m/sec.

The empirical Equation (7.1) gives

$$V_F = 0,44 \ \omega_T \ b \sqrt{(1 - (\frac{\omega_v}{\omega_T})^2) \sqrt{\frac{\nu}{\mu}}} =$$

$$0,44\cdot 4,96\cdot 10,3 \sqrt{(1 - 0,161) \frac{\sqrt{0,95}}{0,o239}} = 131 \text{ m/sec.}$$

Critical velocities in coupled oscillations: Diagrams Fig.'s 31-33, Eq. (7.2)

$d/b = \frac{0,4}{10,3} = 0,o39$; $V = V_F \ k$; $\frac{\omega_T}{\omega_v} = 2,49$

	$\alpha = 0°$	$\alpha = \pm 5°$	$\alpha = \pm 10°$
V_1 =	130 · 0,58 = 75 m/sec	· 0,3o = 39 m/sec	· 0,142 = 18 m/sec
V_2 =	0,55 = 71 "	0,37 = 48 "	0,27 = 35 "
V_3 =	0,49 = 46 "	0,43 = 56 "	0,32 = 42 "

The amplitudes ϕ will be increased by the factor

$$\sqrt{\frac{\mu}{0,o18}} \cdot \sqrt{\frac{1,1}{\nu}} = 1,2o$$

in radians $\phi_1 = 0,o12$; $\phi_2 = 0,12$; $\phi_3 = 0,24$

or $\phi_1 = 0,69°$; $\phi_2 = 6,9°$; $\phi_3 = 13,8°$

Critical velocities in vertical oscillations. Diagram Fig. 42, Eq. (7.6). Area for small oscillations

$V_c = b \ \omega_v \ k_v = 10,3\cdot 1,99\cdot (0,25 - 0,41) = 5,6$ -9 m/sec

amplitude $< 0,01 \cdot 1,15$ b $\approx 0,12$ m

Increasing oscillations

$V_c = b \cdot 1,99 \cdot 3,7 = 76$ m/sec (amplitude = 0 m)

$V_c = b \cdot 1,99 \cdot 4,0 = 82$ m/sec (amplitude = 1,2 m)

Amplitude will be increased by the factor: $\sqrt{\frac{\mu}{0,018}} = 1,15$, and $V_c = 82$ m/sec corresponds to the amplitude $a = 0,1 \cdot b \cdot 1,15 = 1,2$ m.

As will be seen the bridge is reasonable stable against coupled oscillations, compare Chapt. 8. Small vertical oscillations will take place for winds between 5 - 9 m/sec and the lowest mode of oscillation. For velocities of 9 - 14 m/sec such oscillations will take place in the second mode of oscillation $\omega_v = 3,12$ and so on.

Small vertical oscillations with amplitudes less than $\pm$ 0,1 m will take place frequently on this bridge. The oscillations will be without any harmfull effect to the bridge and usually the amplitude will be only a fraction of $\pm$ 0,1 m. This amplitudes will clearly be felt by pedestrians, but should not be alarming to them.

Above is given the results for symmetrical oscillations. The antimetrical ones will have to be calculated in a similar manner. However, for this special bridge the symmetric oscillation will be the critical one, giving the lower values of wind velocity.

8. NATURAL WIND AND WIND FORCES.

8.1. Nature of wind.

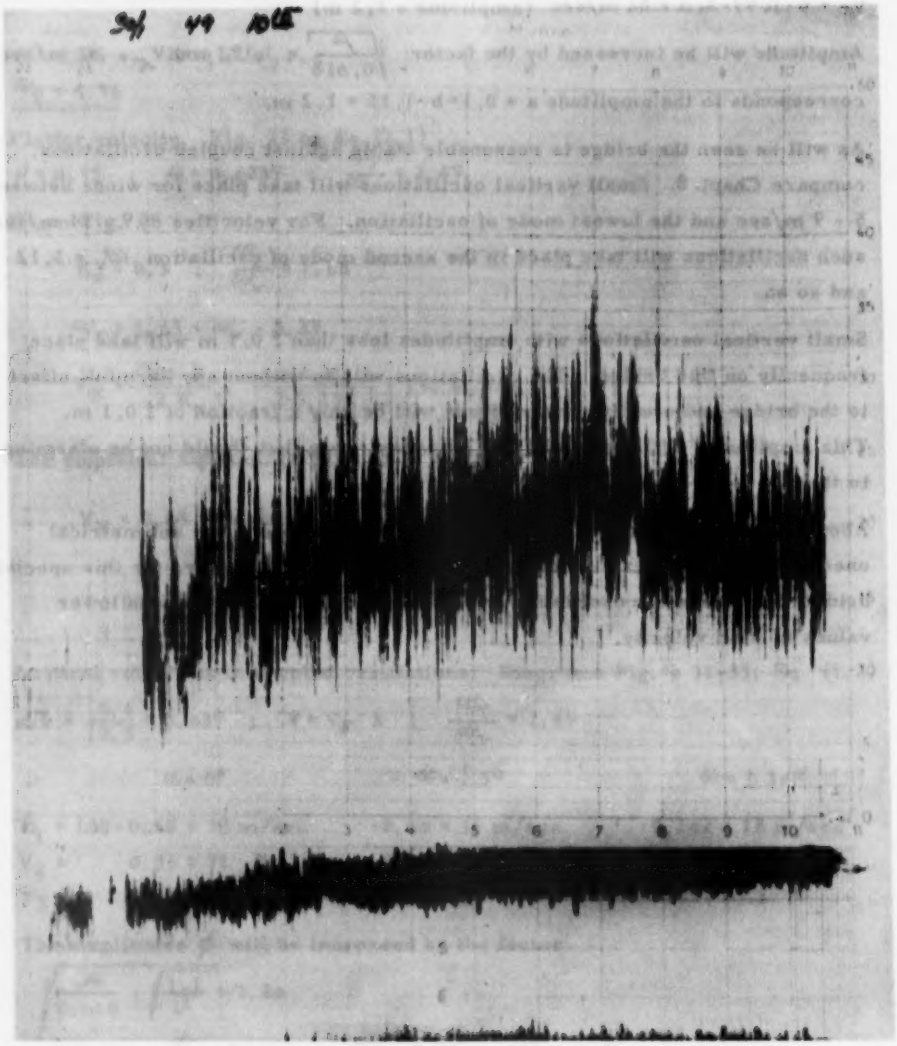

Fig. 45. Variation of wind velocity and wind direction during a storm.

The nature of the wind is little known, however, some investigations have been made [20, 21].

The wind velocity and the wind direction are varying, and the peaks in wind velocity, gusts, exist usually only a few seconds.

The turbulence of the wind is due to the roughness of the earth surface and the mixing of warm and cold air. This form of turbulence will be impossible to produce in a wind tunnel. The best verification of our theories and wind tunnel tests is the behaviour of the existing suspension bridges.

In the opinion of the author the correlation between the bridges and the model tests is good. To the authors knowledge there has never been reported any trouble by bridges which should be safe predicted by model tests. In Fig. 45 is represented the wind measuring during a small storm, in Bergen. The variation in wind velocities is substantial, however, the gusts are all of short time, some seconds to a few minutes. The variation in vertical direction is not measured, in horizontal direction the variation is frequently $\pm 45^{o}$ and any tale of a steady wind is impossible.

8.2. Design wind velocity.

The upper limit of wind velocity is non-existent. However, we pretty well know the chance for getting a given velocity. A reasonable criterion for the design should be the wind velocity reached once in a hundred year. Bridges and buildings have to stand this pressure even if the duration of it is just a few seconds. A wind velocity of 65 m/sec inclusive gust, as used for instance in Norway, is a reasonable velocity, perhaps on the conservative side.

In the investigation of aerodynamic stability we have to remember that the time for starting and building up of a dangerous oscillation will be dependent on the size of the bridge. The time will be of magnitude 5 min - 10 min - 15 min.

Remembering this it seems to be reasonable to calculate with a mean wind velocity. For instance if the static wind incl. gust is represented by 65 m/sec, the bridge should be aerodynamically stable for a velocity of 50 m/sec, smaller bridges perhaps 55 m/sec.

An average wind of 50 m/sec, lasting for several minutes and uniform over the entire span of the bridge will be somewhat more unique than the maximum design load on a bridge or a maximum wind gust on a building or a usual bridge with girder or truss spans.

The location of the bridge is very important. Gust velocity of 65 m/sec or mean wind velocity 50 m/sec may occure on a bridge which stands high above

sea or valley level and with few natural obstructions to decrease the wind. A bridge running just a few meters above sea or river level will never have winds of this magnitude, velocities of 30 m/sec, and 25 m/sec resp. seem to be sufficient for a bridge thus situated.

A very mountanous terrain with narrow valleys may give a specially strong turbulence and high gust factors. Bridge oscillations started by the static deformation due to a wind gust blowing quer to the valley have been observed some times in Norway. However, these oscillations have died rapidly out as the wind, with the ever changing direction and velocity, is unable to support the oscillations.

REFERENCES.

The references given below are no complete list of papers conserning aerodynamic stability of suspension bridges. The references represent the papers which have been of any importance to this work.

1. The Failure of the Tacoma Narrows Bridge. Bulletin No. 78. School of Eng. Tex. Eng. Exp. Stat., 1944.

2. Farquharson, Vincent: Aerodynamic Stability of Suspension Bridges. Bull. No. 116. Part I-V. Univers. o. Wash. Eng. Exp. Stat., 1949-54.

3. Bleich, McCullough, Rosecrans, Vincent: The Matematical Theory of Vibration of Suspension Bridges. Bureau of Public Road. Department of Commerce, Wash., 1950.

4. F. Bleich: Dynamic Instability of Truss-Stiffened Suspension Bridges under Wind Action. A. S. C. E. Trans. Vol. 114, 1949.

5. F. Bleich: Structural Damping in Suspension Bridges. A. S. C. E. Trans., Vol. 117, 1952.

6. R. A. Frazer, C. Scruton: A Summarised Account of the Severn Bridge Aerodynamic Investigations. Report N. P. L. /Aero/222. Nat. Phys. Lab., 1952.

7. C. Scruton: An Experimental Investigation of the Aerodynamic Stability.. 3. Congress. I. A. B. S. E. Prelim. Publ. Liege, 1948.

8. D. B. Steinman: Rigidity and Aerodynamic Stability ... A. S. C. E. Trans., Vol. 110, 1945.

9. D. B. Steinman: Aerodynamic Theory of Bridge Oscillations. A. S. C. E. Trans., Vol. 115, 1950.

10. A. Selberg: Design of Suspension Bridges. D. K. N. V. S.: Trondheim, 1946.

11. A. Selberg: Suspension Bridges with Cables Fastened .. I. A. B. S. E. Publ., Vol. 8, Zürich, 1947.

12. A. Selberg: Beregning av små hengebruer. Bygningsstatiske Meddelelser, København 1949.

13. A. Selberg: Dampening Effect in Suspension Bridges. I. A. B. S. E. Publ., Vol. 10, Zürich, 1950.

14. A. Selberg: Calculation of Lateral Truss .. I. A. B. S. E. Publ., Vol. 7, Zürich, 1943/44.

15. A. Selberg: Discussion to paper by I. K. Silverman. The Lateral Rigidity . . A. S. C. E. Proc. Paper 1520, 1958.

16. Farquharson: Model Verification of the Classical Flutter Theory . . I. A. B. S. E., Publ. Vol. 12, Zürich, 1952.

17. G. S. Vincent: Mathematical Prediction of Suspension Bridge Behaviour . I. A. B. S. E. Publ. Vol. 12, Zürich, 1952.

18. T. Teordorsen: General Theory of Aerodynamic Instability and the Mechanism of Flutter. N. A. C. A. Tec. Rep. No. 496. Wash., 1935.

19. T. v. Karman, W. R. Sears: Airfoil Theory for Non-Uniform Motion. Jour. Aero. Sc., 1958.

20. M. Jensen: Aerodynamik i den naturlige vind. Teknisk Forlag, København, 1959.

21. M. Sherlock: Nature of the Wind. A. S. C. E. Proc., Paper 1708, 1958.

SUMMARY.

The aim of this paper is to give the bridge designer a tool for an investigation of the aerodynamic stability of suspension bridges. To facilitate the reading of the paper the presentation, when possible, follows the methods of statics and the deflection theory of suspension bridges. Methods which are familiar to the bridge designers.

The first part of the paper deduce equations for vertical and torsional oscillations, and results in some very simple formulae for the calculation of natural frequencies and modes of oscillation, see Chapt. 2 and 3. In these formulaes are included the effect of inclination of the suspenders. As will be seen from Fig. 5 this effect is quite important for oscillations with 2 half waves in a span.

Investigation of warping resistance and torsional stiffness of bridges with lateral trusses at upper and lower chord of stiffening truss, results in formulae suitable for calculation of frequencies, see Chapt. 3.

The second part of the paper gives the necessary equations for dimensioning of section models for wind tunnel tests. A brief reference is given of the flutter theory and the resulting critical wind velocity, see Fig. 25.

A description of some model investigations on Norwegian suspension bridges is given. In connection with these tests a systematic model investigation of some typical bridge sections was made -, resulting in diagrams, Fig.'s 30-38, which give the critical velocity with good accuracy when the frequencies are known for coupled oscillations.

Vertical oscillations may be investigated with use of the diagrams Fig.'s 42-44.

As may be seen from the numerical example, Chapt. 7. 7, small, harmless vertical oscillations will occure on suspension bridges. The importance of this type of oscillations is, however, usually overestimated, they will be felt only by the pedestrians.

When the Tacoma Bridge disaster occured, the knowledge of these problems among bridge designers was almost Zero. The lessons of the many disasters in the last century had been forgotten. To-day the investigation of aerodynamic stability should be a selfevident part of the design of any suspension bridge. In the opinion of the author a sufficiently accurate value of the critical wind velocity for most bridges may be found with use of the diagrams presented here.

ooOoo

THE LAST VOLUMES OF ACTA POLYTECHNICA

Civil Engineering and Building Construction Series

(The predecessor of Acta Polytechnica Scandinavica)

Volume 4

Nr 1 LANGE HANSEN, P: *The Plastic Theory of Curved Beams with Compressive Axial Forces.* Acta P 215 (1957). 32 pp. Sw. Kr 5: 00 UDC 624.072.3:539.214

Nr 2 ISAKSSON, Å: *Creep Rates of Excentrically Loaded Test Pieces.* Acta P 219 (1957). 33 pp. Sw. Kr 4: 50 UDC 620.172.251.2

Nr 3 IDORN, G M: *Concrete Deterioration of a Foundation.* Acta P 221 (1957). 48 pp. Sw. Kr 8: 00 UDC 620.163.24:693.5

Nr 4 ORDING, F BOYE: *Die Beständigkeit der Basislatten.* Acta P 225 (1957). 16 pp. Sw. Kr 7: 00 UDC 526.25

Nr 5 SUNDSTRÖM, E: *Creep Buckling of Cylindrical Shells.* Acta P 230 (1957). 34 pp. Sw. Kr 5: 00 UDC 539.434.624.074.4:434.1

Nr 6 KUDSK-JØRGENSEN, B: *Calculation of Time-Concentration Curves in a Stationary, Laminar Liquid Flow Through a Circular-Cylindrical Tube.* Acta P 233 (1957). 18 pp. Sw. Kr 5: 00 UDC 532.517.2:612.13

Nr 7 ENGELUND, F: *On the Theory of Multiple-Well Systems.* Acta P 234 (1957). 11 pp. Sw. Kr 5: 00 UDC 551.495.54

Nr 8 BRINCH HANSEN, J: *Calculation of Settlements by Means of Pore Pressure Coefficients.* Acta P 235 (1957). 14 pp. Sw. Kr 5: 00 UDC 624.131.526

Nr 9 DAHL, N J: *On Water Supply from Wells.* Acta P 236 (1957). 17 pp. Sw. Kr 5: 00 UDC 551.49:628.112

Nr 10 LUNDGREN, H: *Dimensional Analysis in Soil Mechanics.* Acta P 237 (1957). 32 pp. Sw. Kr 6: 00 UDC 624.131

ACTA POLYTECHNICA SCANDINAVICA

Civil Engineering and Building Construction Series

Ci 1 BRETTING, A E: *Stable Channels.* (Acta P 245/1958). 130 pp. Sw. Kr 7: 00 UDC 626.01:627.1

Ci 2 OSTERMAN, J: *Notes on the Shearing Resistance of Soft Clays.* (Acta P 263/1959) 24 pp. Sw. Kr. 7.00 UDC 624.131.222

Ci 3 EIDE, OWE AND JOHANNESEN, IVAR J: *Measurement of Strut Loads in the Excavation for Oslo Technical School.* (Acta P 266/1960) 14 pp. Sw. Kr. 7.00 UDC 624.131.532:624.134.4

Ci 4 JOHANNESEN, IVAR J: *Test Section and Installation of Test Equipment, Oslo Subway* and ØIEN KJELL: *An Earth Pressure Cell for use on Sheet Piles* (Acta P 267/1960) 16 pp. Sw. Kr. 7.00 UDC 624.131.386:624.134.4

Ci 5 KJÆRNSLI, BJØRN: *Test results, Oslo Subway* (Acta P. 268/1960) 11 pp. Sw. Kr. 7.00 UDC 624.131.532:624.134.4

Ci 6 KYRKLUND, HARALD: *Über die Einschätzung von Biegespannungen in gekrümmten Balken.* (Acta P. 274/1960) 56 pp. + fig. Sw. Kr. 7: 00 UDC 624.072.7

Ci 7 VUORELAINEN, O: *Thermal Conditions in the Ground from the viewpoint of Foundation Work, Heating and Plumbing Installations and Draining.* (Acta P. 277/1960) 40 pp. Sw. Kr. 7: 00 UDC 624.131.436 + 551.525

Ci 8 VUORELAINEN, O: *The Temperature Field Produced in the Ground by a Heated Slab Laid direct on Ground, and the Heat Flow from Slab to Ground.* (Acta P. 278/1960) 59 pp. Sw. Kr. 7: 00 UDC 536.2:697.133:69.025.1

Ci 9 VUORELAINEN, O: *The Temperatures under Houses Erected Immediately on the Ground and the Heat Losses from their Foundation Slab.* (Acta P. 289/1960) 105 pp. Sw. Kr. 14: 00 UDC 536.2:697.133:69.025.1

Ci 10 GIBSON, R. E. AND LO, K. Y: *A Theory of Consolidation for Soils Exhibiting Secondary Compression.* (Acta P. 296/1961) 16 pp. Sw. Kr 7: 00 UDC 624.131.542:624.131.526

Price Sw. Kr. 7.00

A.s Nidaros og Trøndelagen
Trondheim